

# Identification of a mesenchymal-related signature associated with clinical prognosis in glioma

Zhengwei Zhang<sup>1,2,\*</sup>, Jie Chen<sup>1,2,\*</sup>, Xiuhao Huo<sup>1,2</sup>, Gang Zong<sup>1,2</sup>, Kebin Huang<sup>1,2</sup>, Meng Cheng<sup>1,2</sup>, Libo Sun<sup>1,2</sup>, Xiaoyu Yue<sup>1,2</sup>, Erbao Bian<sup>1,2,&</sup>, Bing Zhao<sup>1,2</sup>

<sup>1</sup>Department of Neurosurgery, The Second Affiliated Hospital of Anhui Medical University, Hefei 230601, China

<sup>2</sup>Cerebral Vascular Disease Research Center, Anhui Medical University, Hefei 230601, China

\*Equal contribution

**Correspondence to:** Bing Zhao, Erbao Bian; email: [aydzhb@126.com](mailto:aydzhb@126.com), <http://orcid.org/0000-0002-5758-4559>; [aydbeb@126.com](mailto:aydbeb@126.com)

**Keywords:** glioma, mesenchymal, gene signature, prognosis, proliferation

**Received:** November 30, 2020

**Accepted:** March 4, 2021

**Published:** April 19, 2021

**Copyright:** © 2021 Zhang et al. This is an open access article distributed under the terms of the [Creative Commons Attribution License](https://creativecommons.org/licenses/by/3.0/) (CC BY 3.0), which permits unrestricted use, distribution, and reproduction in any medium, provided the original author and source are credited.

## ABSTRACT

Malignant glioma with a mesenchymal (MES) signature is characterized by shorter survival time due to aggressive dissemination and resistance to chemoradiotherapy. Here, this study used the TCGA database as the training set and the CGGA database as the testing set. Consensus clustering was performed on the two data sets, and it was found that two groups had distinguished prognostic and molecular features. Cox analysis and Lasso regression analysis were used to construct MES signature-based risk score model of glioma. Our results show that MES signature-based risk score model can be used to assess the prognosis of glioma. Three methods (ROC curve analyses, univariate Cox regression analysis, multivariate Cox regression analysis) were used to investigate the prognostic role of texture parameters. The result showed that the MES-related gene signature was proved to be an independent prognostic factor for glioma. Furthermore, functional analysis of the gene related to the risk signature showed that the genes sets were closely related to the malignant process of tumors. Finally, FCGR2A and EHD2 were selected for functional verification. Silencing these two genes inhibited the proliferation, migration and invasion of gliomas and reduced the expression of mesenchymal marker genes. Collectively, MES-related risk signature seems to provide a novel target for predicting the prognosis and treatment of glioma.

## INTRODUCTION

Glioma mainly occurs in the brain and glial tissue, and is the most common primary malignant brain tumor in adults [1, 2]. Gliomas are astrocytes, oligodendrocytes, or a mixture of these two cell types. Gliomas are classified into four categories (grades I~IV) based on malignancy and overall survival (OS) by the International Classification of Diseases–Oncology, version 3 (ICD-O-3) and the World Health Organization (WHO). Among them, grade IV glioma (glioblastoma) has a very poor prognosis, with a median survival between 14.5 and 16.6 months [3, 4]. Even after

surgery, radiotherapy and chemotherapy, the survival time of patients with glioma is only extended by a few months [5]. Therefore, there is an urgent need for accurate prognostic prediction and new therapeutic targets for glioma treatment.

Glioblastoma is the most common primary malignancy in the central nervous system and is fast-growing (grade 4 glioma) [6, 7]. The new classification of GBM (glioblastoma multiforme) tumor subtypes is based on The Cancer Genome Atlas (TCGA) on related genetic mutations, changes in the associated recurrent gene copy number and comprehensive genome sequence analysis.

GBM is divided into proneural, neural, classical and mesenchymal subtypes according to different biological, imaging and clinical characteristics [8, 9]. High-grade glioma (HGG) can also be divided into three subtypes: proneural (PN), mesenchymal (MES) and proliferative (Prolif) because of their different molecular characteristics, including CHI3L1 / YKL40, SERPINE1 and PDPN. The MES subtype is a more malignant form with a higher tendency for relapse, metastasis, and increased vascularity [10–12]. MES related to a consistently poor prognosis with a median survival time of 1.2 years [11]. GBM relapse has been verified to be closely associated with mesenchymal, stem-like phenotypes that are resistant to treatment [13, 14]. Mesenchymal GBMs showed the highest percentage of microglia, macrophage, and lymphocyte infiltration, which was connected with a worse prognosis [15].

In recent years, central nervous system tumors have been reclassified, which has produced a paradigm shift in personalized therapeutics and prognostic factor-guided treatment decisions [6]. Recently, it has been proposed that the prognosis of glioma is closely related to immune-related lncRNAs, N6- methyladenosine-related lncRNAs and energy metabolism-related genes [16–18]. Therefore, we speculate that the detection of MES-related genes is of great significance for evaluating prognosis. In addition, these findings may contribute to the discovery of prognostic biomarkers for glioma and the development of more accurate treatment processes.

This study used TCGA and Chinese Glioma Genome Atlas (CGGA) RNA sequencing data to study the clinical value of MES-related genes from the TCGA and Ivy Glioblastoma Atlas Project (Ivy GAP) databases.

According to the expression levels of MES-related genes, the patients were divided into two groups by consensus clustering analysis, and there were significant differences in prognosis and molecular characteristics. Then, Lasso regression was used to calculate the regression coefficient, and the risk score was calculated based on the regression coefficient and the gene expression level. The patients were graded into high-risk and low-risk groups of the median risk score, in which the low-risk group had a better prognosis than the high-risk group. The MES-related signature is closely related to the prognosis of patients and could act as an independent pathological predictive factor. Furthermore, functional analysis showed that gliomas with a higher risk score for MES-related genes were associated with many aspects of glioma progression, including epithelial-mesenchymal transition, angiogenesis, hypoxia and inflammatory response. Subsequent cell function test results showed that inhibition of FCGR2A or EHD2 significantly represses proliferation, migration, and invasion of glioma cells, and reduces the expression of mesenchymal marker genes. Therefore, these results suggest that MES-related genes will be better for predicting the prognosis of glioma and provide novel targets for glioma treatment.

## RESULTS

### Fifteen MES-related genes from the TCGA and Ivy GAP databases

The MES-related genes were obtained from the TCGA and Ivy GAP databases. As shown in Figure 1A, the Venn diagram showed a total of 21 intersecting genes, including EFEMP2, CHI3L1, TIMP1, EMP3, NRP1, EHD2, HK3, RRAS, FES, PTRF, MYH9, MVP,

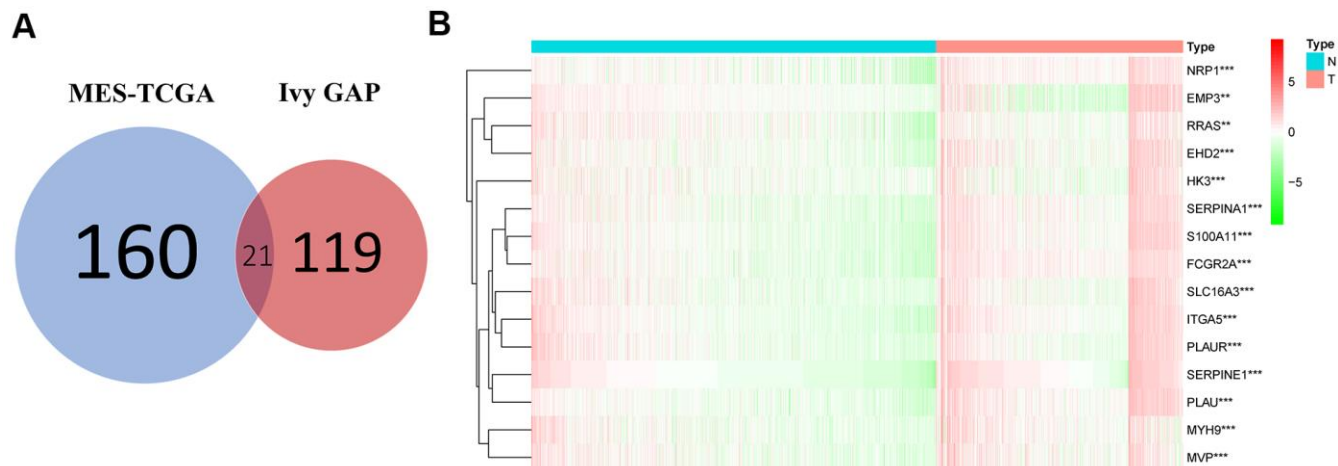


**Figure 1. Acquisition and verification of MES-related genes.** (A) Venn diagram indicating that 21 MES-related genes were selected from the Ivy GAP and TCGA databases. (B) The heat map shows that 15 of the MES-related genes were significantly different between the normal and tumor groups. \*\*P < .01; \*\*\*P < 0.001.

SERPINA1, S100A11, THBD, FCGR2A, SLC16A3, ITGA5, and PLAU. Then, we used differential gene analysis to identify differentially expressed genes between the normal and tumor groups, 15 of which had significant differences between the two groups, including NRP1, EMP3, FCGR2A, PLAUR, SERPINA1, SERPINE1, MYH9, S100A11, MVP, RRAS, ITGA5, SLC16A3, EHD2, PLAU, and HK3, and all had a positive correlation (Figure 1B and Table 1).

### **Stratification of gliomas based on the fifteen MES-related genes**

Consensus clustering of 650 samples identified two clusters. In the TCGA data set, the cluster stability increased between  $k = 2$  and  $k = 9$ . Next, we observed significant differences in the clinical and molecular characteristics of the two clusters identified by consensus clustering (Figure 2A–2C and Supplementary Figure 2A). In the training cohort, cluster 1 was closely related to the age at diagnosis and grade of glioma, as well as the type of glioma ( $p < 0.001$ ) (Figure 2D). Similarly, these results were verified in the CGGA database (Supplementary Figure 2B–2F). In addition, we observed that the overall survival (OS) of cluster 2 was significantly shorter than cluster 1 (Figure 2E). At the same time, the CGGA validation set clearly showed the same results in the two different prognostic subgroups (Figure 2F). These results indicate that the MES-related gene set is related to the survival time of patients with glioma, and cluster 2 is much shorter than cluster 1.

### **Establishment of the MES-related gene risk signature**

The predictive value of the risk score model was evaluated using the TCGA data set as the training set. To establish the MES-related gene signature, first, univariate Cox regression analysis of all data from the training and testing cohorts was used to select six genes from 15 MES-related genes. We chose six genes as risk coefficients in the model because these six genes had higher hazard ratios (Figure 3A). Then, through the Lasso regression algorithm, six genes were designated as active covariates to gauge the prognostic value and obtain the correlation coefficients of each gene (Figure 3B). Next, the risk score of the patients was calculated by the correlation coefficients and gene expression. The training set was segmented into high-risk and low-risk groups based on their median risk score to verify the performance of the risk score as a classifier for evaluating characteristic genes. We found clinically significant differences and different molecular characteristics between the high- and low-risk groups (Table 2). The high-risk group had an older age, a higher glioma grade, and a more malignant glioma type than the low-risk group (Figure 3C).

To verify whether the MES-related risk characteristics are equally applicable in another sample, we developed a risk score for each patient in the CGGA database according to the risk score of the training set. Consistent with the above results, compared with low-risk groups, high-risk groups tend to have more malignant clinical features. In general, we still found important differences between the two clusters in the independent verification group (Supplementary Figure 3A–3C).

### **The 6-gene signature shows strong prognostic power**

The overall survival rate of patients in the low-risk group was significantly longer than that of patients in the high-risk group by Kaplan-Meier analysis (Figure 4A). In addition, patients in the low-risk group had a significantly positive progression-free survival time compared to the high-risk group (Supplementary Figure 4A). To verify whether the risk coefficient is an independent prognostic factor for the prognosis of glioma, we carried out univariate and multivariate Cox regression analyses. The risk score was not associated with age, sex, grade, or subtype, but it was significantly related to the patient's OS and was an independent prognostic factor (Figure 4C, 4D). Additionally, the ROC curve was used to further evaluate the specificity and sensitivity of the risk score as a predictor by calculating the AUCs (areas under the curve) of the risk score for 1-, 3- and 5-year OS. The AUC values of the risk score were 0.844, 0.882 and 0.863, which showed its powerful ability to predict prognosis (Figure 4E).

In CGGA, the same results were obtained. Overall survival analysis showed that low-risk patients also had a better prognosis (Figure 4B). We performed univariate and multivariate Cox regression analyses of the CGGA data set, which revealed that the risk score was an independent prognostic factor (Supplementary Figure 4B, 4C). The ROC curve analysis also showed good specificity and sensitivity for one-, three-, and five-year survival predictions, and the one-, three-, and five-year AUC values were 0.813, 0.815 and 0.723, respectively (Figure 4F).

### **Functional analysis of the 6-MES related genes**

To explore the functional characteristics of potential changes associated with the 6-gene signatures, gene set enrichment analysis (GSEA) was performed between the high- and low-risk score groups. We discovered that the high-risk group was closely related to epithelial-mesenchymal transition, angiogenesis, inflammation, and hypoxia compared to the low-risk group (Figure 5A–5D). Additionally, we performed GO analysis to explore the correlation of the difference function between the high- and low-risk groups. Similarly, we

**Table 1. Full names of the 15 related genes and their p-values.**

Gene symbol	Gene name	p value
SERPINE1	Serpin Family E Member 1	9.48E-98
S100A11	S100 Calcium Binding Protein A11	8.36E-82
ITGA5	Integrin Subunit Alpha 5	3.54E-69
HK3	Hexokinase 3	3.55E-04
RRAS	RAS Related	9.32E-03
FCGR2A	Fc fragment of IgG receptor IIa	2.84E-108
PLAU	Plasminogen Activator, Urokinase	2.72E-114
SERPINA1	Serpin family A member 1	1.53E-74
MYH9	Myosin Heavy Chain 9	1.44E-47
NRP1	Neuropilin 1	2.71E-71
PLAUR	Plasminogen Activator, Urokinase Receptor	1.73E-23
EHD2	EH Domain Containing 2	1.87E-30
EMP3	Epithelial Membrane Protein 3	2.35E-03
MVP	Major Vault Protein	1.00E-39
SLC16A3	Solute Carrier Family 16 Member 3	2.29E-32

discovered that the positively related genes were mainly enriched in cell adhesion molecule binding, tumor necrosis factor receptor superfamily binding, and tubulin binding (Figure 5E), which are closely associated with the epithelial-mesenchymal transition process. Next, KEGG analysis verified that the high-risk group was closely related to focal adhesion and cell adhesion molecules (Figure 5F). We found that these genes may be involved in these processes. Leading to a worse prognosis for patients with glioma.

#### **Inhibiting FCGR2A or EHD2 expression could significantly suppress glioma proliferation, migration, and invasion**

Using the database to analyze the gene differences between the normal group(n=1108) and glioma group(n=650), it was also found that these six genes are different except for EMP3. Next, TCGA database was utilized to analyze the overall survival and disease-free survival rate of the six genes between the high-expression group and the low-expression group. We found that glioma patients with high expression levels of these genes had a worse prognosis than those with low expression levels (Figure 6 and Supplementary Figure 5). Subsequently, we analyzed these six genes and found that among them, FCGR2A and EHD2 have rarely been studied in glioma, and there are no functional tests. Hence, we chose these two genes for functional analysis in glioma. Using five existing glioma cell lines in the research group to carry out qRT-PCR, it was found that FCGR2A was expressed at a relatively high level in LN18 and T98G cells, whereas EHD2 was expressed at

a high level in U251 and SNB19 cells (Figure 7A, 7B). To verify the effects of these two genes on the proliferation, migration and invasion of glioma cells, the genes were silenced with siRNAs. Three fragments of siFCGR2A (siFCGR2A(pro)) and siEHD2-2 were selected to silence genes in LN18 and U251 cells (Figure 7C, 7D) and were verified in T98G and SNB19 cells (Supplementary Figure 6A, 6B). Functional tests were performed on the cell lines corresponding to these two genes, including the MTT assay, colony formation assay, Transwell assay and Matrigel invasion assay. The MTT assay showed that cell proliferation viability was significantly inhibited at 24 h, 36 h, 48 h and 72 h after transfection (Figure 8A, 8B and Supplementary Figure 7A, 7B). After the colony formation assay was carried out for approximately ten days, it was found that in glioma cells, the cloning ability of cells strikingly decreased after silencing, but it was difficult for U251 cell lines to form colonies (Figure 8C, 8D and Supplementary Figure 7C–7F). The Transwell and Matrigel invasion assays showed that glioma cells' ability to migrate and invade was significantly reduced after siRNA silencing of the target gene (Figure 8E–8J). These results revealed that silencing FCGR2A or EHD2 reduced glioma cell proliferation, migration and invasion. Through mechanistic studies, it was found that silencing the FCGR2A or EHD2 gene can inhibit the expression of the GBM mesenchymal marker genes CHI3L1 and CD44 (Figure 9A–9D). Further research on MES marker proteins. In our study, we found that CD44, BMI1 and ZEB1 showed different degrees of expression inhibition after FCGR2A and EHD2 were silenced, but VIM did not change significantly (Figure 9E, 9F). We



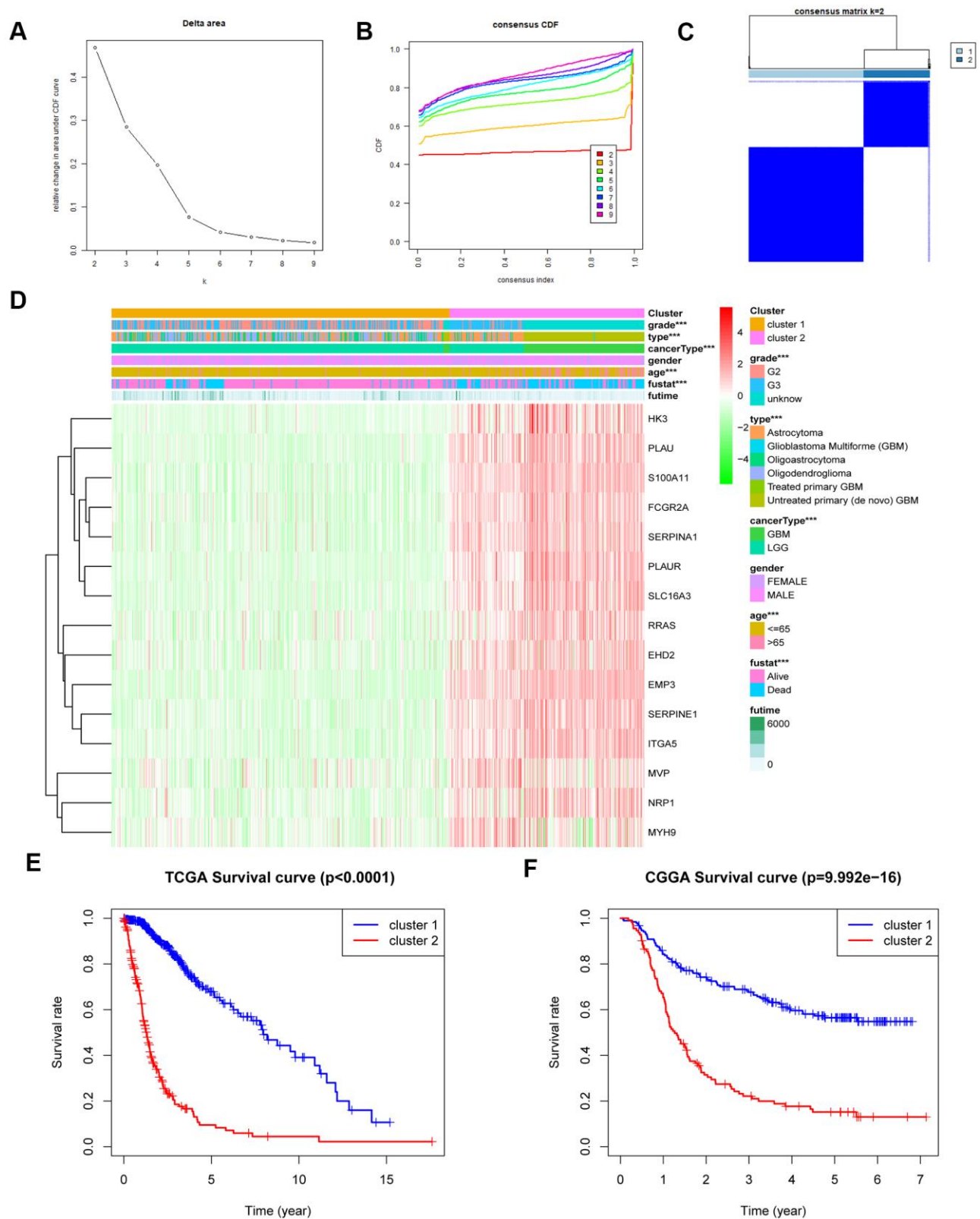


**Figure 2. MES-related gene sets could classify the clinical and molecular features of gliomas.** (A) Relative change in the area under the CDF curve for  $k = 2$  to  $k = 9$ . (B) Consensus clustering CDF for  $k = 2$  to  $k = 9$ . (C) Consensus clustering matrix of 650 samples from the TCGA dataset for  $k = 2$ . (D) Heat map of MES-related genes between cluster 1 and cluster 2 of the TCGA cohort. (E) Survival analysis of patients in cluster 1 and cluster 2 based on TCGA clinical data. (F) Survival analysis of patients in cluster 1 and cluster 2 based on CGGA clinical data. CDF, cumulative distribution function; \*\*\* $P < 0.001$ .

further verified that these genes play an important role in glioma.

## DISCUSSION

Human brain glioma is the most common primary malignant tumor. But the prognosis for patients with these tumors remains poor despite standard care of surgery, radiation therapy and temozolomide chemotherapy [19]. Therefore, it is imperative to

identify potential prognostic and therapeutic targets for glioma. For those facing prognostic evaluation and treatment, many genes have been explored as biomarkers [20], but they are still not enough to predict the convoluted prognosis of glioma alone.

MES is a type of glioblastoma that can be transformed from other types of gliomas [21, 22]. The MES transition can be induced by master transcription factors (TFs), STAT3, C/EBP $\beta$ , and TAZ through the NF- $\kappa$ b

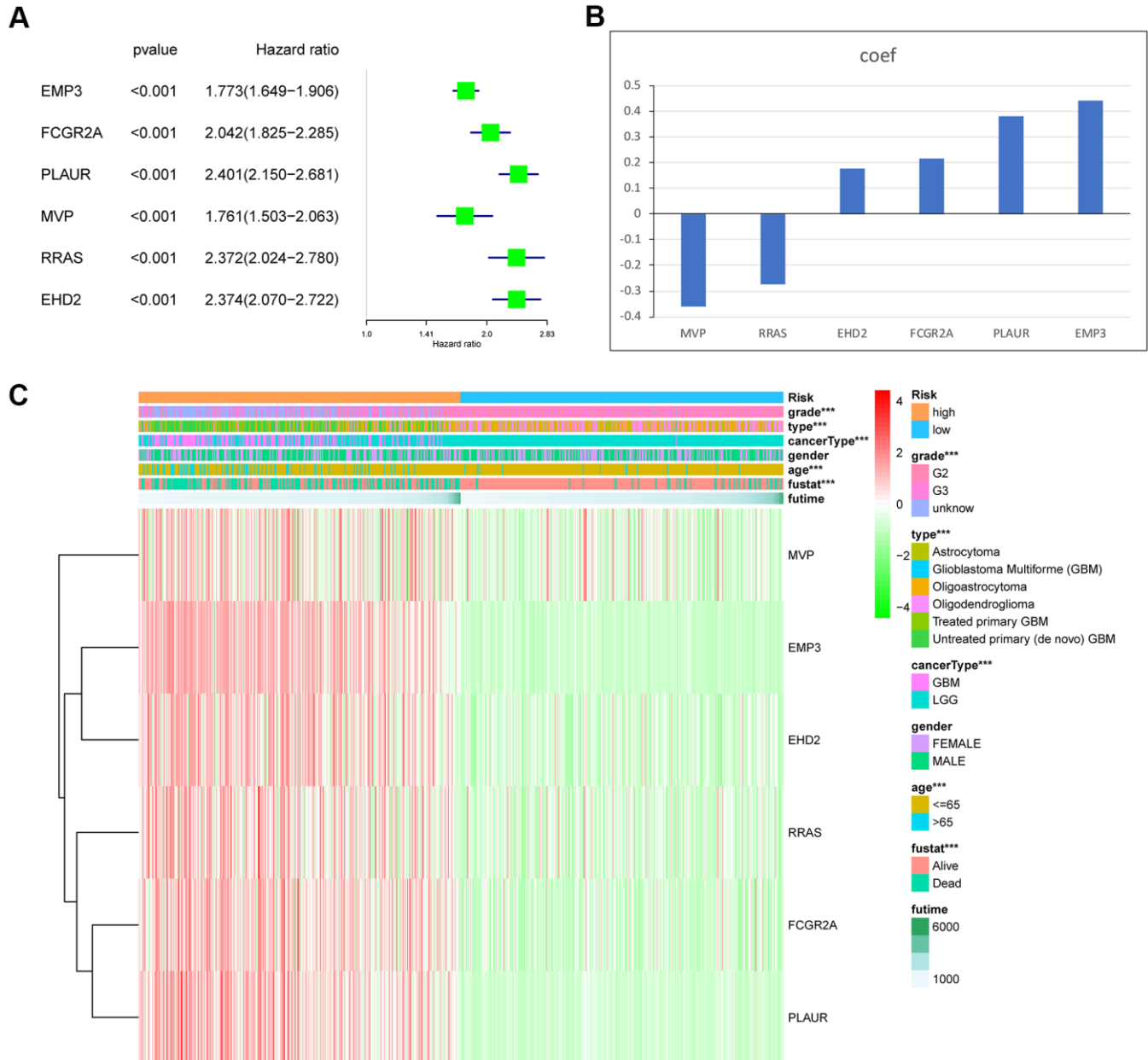


**Figure 3. Identification of the 6-gene risk signature by Lasso regression analysis in the TCGA dataset. (A)** The hazard ratio and P value of the 6 MES-related genes. **(B)** Coefficient values for each of the 6 selected genes. **(C)** Heat map showing the association of risk scores and clinicopathological features. \*\*\*P < 0.001.

**Table 2. Correlation between 6-gene-based risk scores and clinicopathological factors of glioma patients in the two cohorts.**

<b>Training set RNA-seq cohort (n =665)</b>			
<b>Features</b>	<b>Low-risk score</b>	<b>High- risk score</b>	<b>P- value</b>
	<b>n=333</b>	<b>n=332</b>	
Age			
≤ 65	320	258	<b>&lt;0.0001</b>
> 65	13	74	
Gender			
Male	189	194	ns
Female	144	138	
Grade			
II	186	59	<b>&lt;0.0001</b>
III	145	115	
IV	2	158	
Vital status			
Alive	294	152	<b>&lt;0.0001</b>
Dead	39	180	
<b>Testing set RNA-seq cohort(n=280)</b>			
<b>Features</b>	<b>Low-risk score</b>	<b>High- risk score</b>	<b>P- value</b>
	<b>n=165</b>	<b>n=115</b>	
Age			
≤ 65	163	112	ns
> 65	1	2	
Gender			
Male	96	71	ns
Female	69	44	
Grade			
II	98	13	<b>&lt;0.0001</b>
III	30	22	
IV	37	77	
Vital status			
Alive	90	21	<b>&lt;0.0001</b>
Dead	75	94	

The training set RNA-seq cohort comes from the TCGA database and testing set RNA-seq cohort comes from the CGGA database. Ns: no significance; Bold type indicates a statistically significant difference (P value < 0.05).

pathway [23]. MES is the most malignant glioblastoma and has a worse prognosis [24]. On the one hand, it has stronger resistance to treatment than other types of gliomas [25]. This therapeutic resistance may be related to the high expression of inflammation-related genes and NF-κB activation [8], which is consistent with our results. On the other hand, MES is related to recurrent tumors; in recurrent tumors, classic markers of mesenchymal tissues were upregulated, including

CHI3L1, CD44, and STAT3 [22]. Moreover, MES is also related to a growth advantage conferred by either a rapid rate of cell division or enhanced survival of tumor cells afforded by neovascularization [22, 26]. In short, MES is often associated with poor prognosis. Therefore, considering the malignant behaviors of MES GBMs and the analysis of the different results in this paper, we selected MES-related genes as factors to evaluate prognosis.

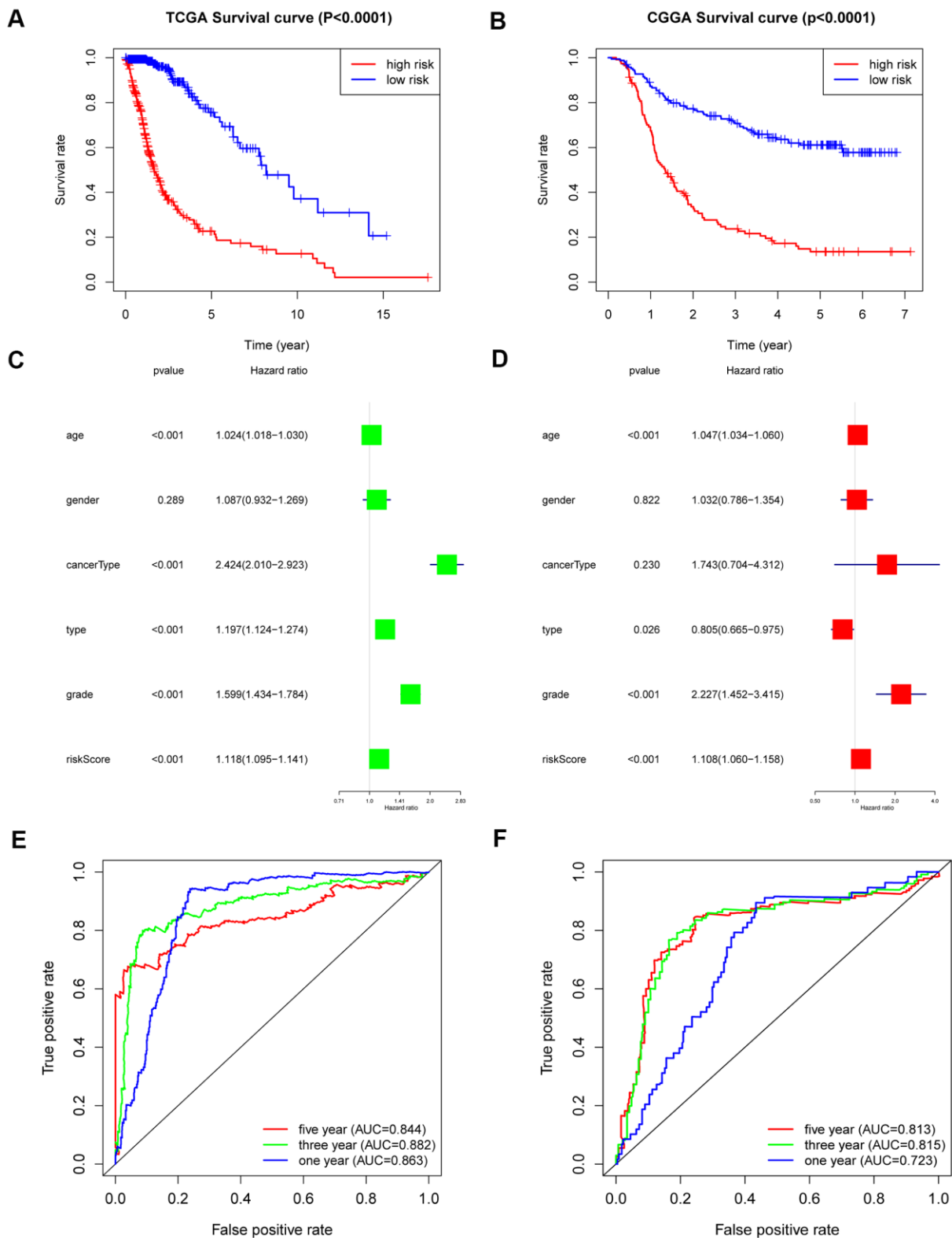


**Figure 4. Outcome prediction of the 6-gene signature in stratified patients of the TCGA cohort and CGGA cohort. (A)** Kaplan-Meier overall survival analysis between the high- and low-risk groups in the TCGA cohort. **(B)** Kaplan-Meier overall survival analysis between the high- and low-risk groups in the CGGA cohort. **(C, D)** Univariate **(C)** and multivariate Cox regression **(D)** analyses of clinical features and the 6-gene-based risk score for OS in the TCGA dataset. **(E)** ROC curves indicating the sensitivity and specificity of predicting 1-, 3- and 5-y survival with the MES-related signature in the TCGA dataset. **(F)** ROC curves indicating the sensitivity and specificity of predicting 1-, 3- and 5-y survival with the MES-related signature in the CGGA dataset.



As previously reported using a model, immune-related genes were successfully selected to predict the prognosis of glioma with a protein expression and mRNA data set from The Cancer Genome Atlas [27].

At the same time, m<sup>6</sup>A methylation, immune-related lncRNA and amino acid metabolism-related genes were used to assess the prognosis of glioma [28–30]. Therefore, we used this model to explore whether

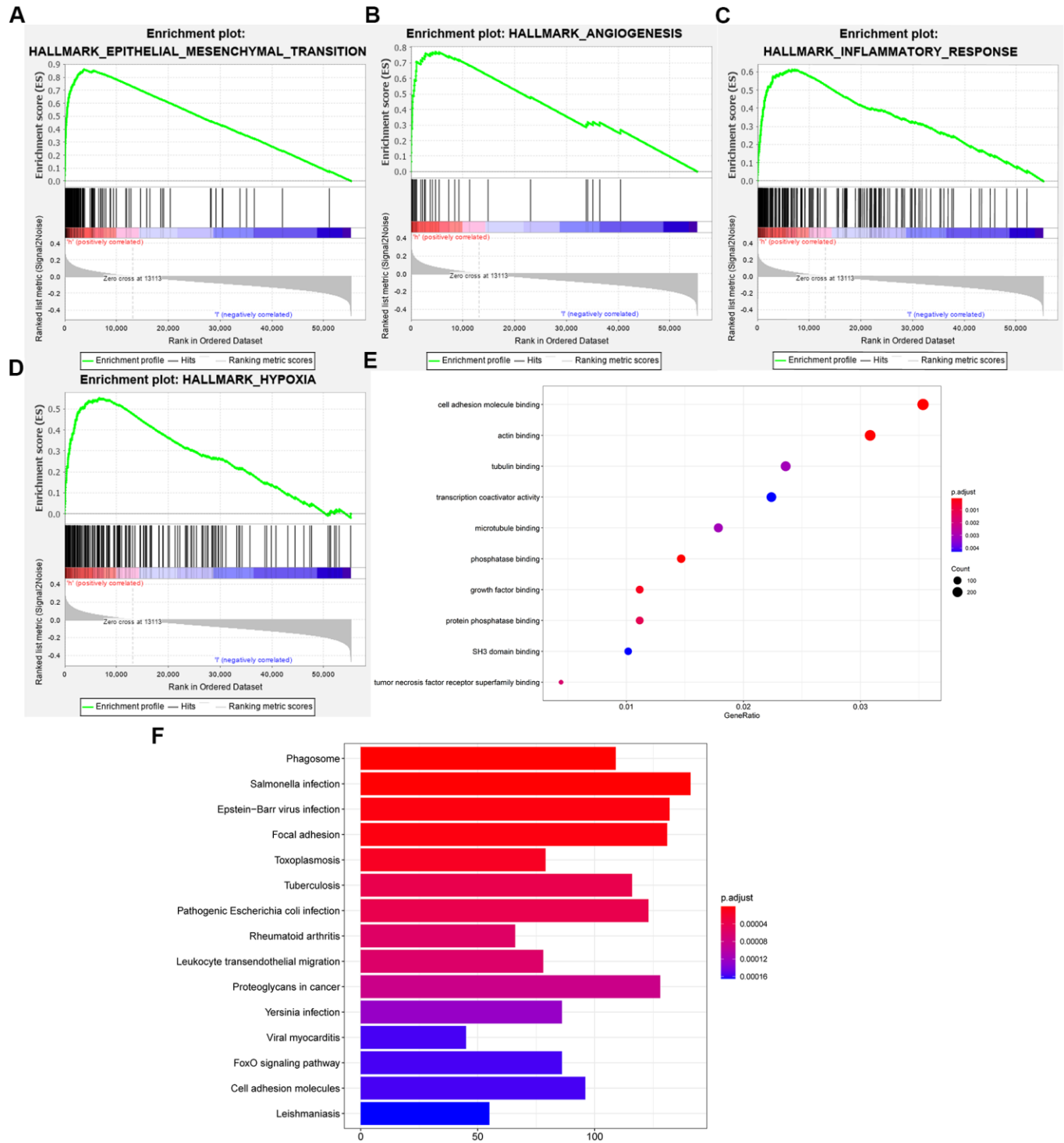


**Figure 5. Functional analysis of the 6-gene signature.** (A–D) GSEA revealed that the two cohorts were enriched for hallmarks of malignant tumors. (E) GO annotations based on the top 4400 genes positively associated with the 6-gene signature. (F) KEGG pathways associated with the risk score.

MES-related genes play a more important role in the prognostic evaluation of glioma. The identification of 21 intersecting genes related to prognosis in the TCGA and Ivy GAP databases was performed as the first step by using the mesenchymal gene set. Then, fifteen genes that were differentially expressed between normal and glioma samples were analyzed and found to be upregulated in the poor prognosis group. Based on a highly reliable survival model, consensus clustering and Lasso regression, which are widely used to generate prognostic genes in the context of high-dimensional data, were applied in this study. We first used the univariate Cox model to screen OS-related genes and applied the Lasso regression model to obtain the regression coefficients. The six genes were obtained to construct a risk score model from the Lasso regression coefficients [31]. The integration of multiple gene markers into a single model was used because the predictive performance of such models can be improved compared to that of a single predictive biomarker. The study found that the risk score model constructed based on TCGA can accurately predict the prognosis of glioma.

Hypoxia-inducible factor-1 $\alpha$  (HIF-1 $\alpha$ ), as the main transcription factor during hypoxia, is significantly upregulated in the MES subtype and plays an important role in tumor angiogenesis and proliferation [32]. Inflammation-related genes are also highly expressed in the MES subtype [8, 33–35]. Epithelial-to-mesenchymal transition is a common pattern of increased malignant behavior and disease progression of epithelial tumors, and the MES phenotype is closely related to this change [25]. This finding supports our GSEA results. Compared with the low-risk group, the high-risk group showed enrichment in the biological processes of epithelial-mesenchymal transition, angiogenesis, inflammation and hypoxia. Similarly, GO and KEGG analyses showed that MES-related genes are closely related to cell adhesion-related processes. These processes are closely related to cancer progression and involve EMT, tumor angiogenesis and the development of an inflammatory tumor microenvironment [35–37]. Consequently, MES-related genes are associated with a higher degree of malignancy and poorer prognosis in gliomas.

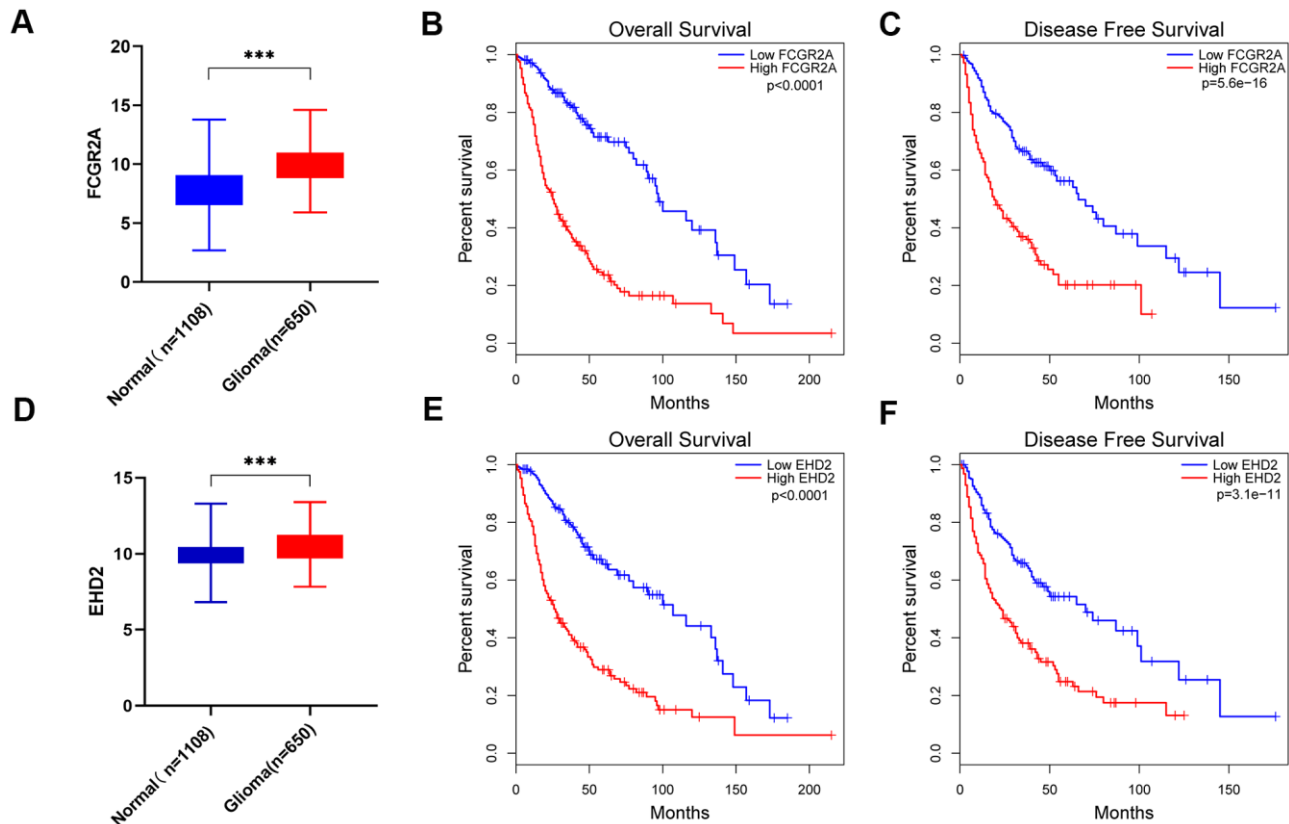


**Figure 6. FCGR2A and EHD2 were selected from the six MES-related genes. (A)** Differences in FCGR2A expression between the normal group and the glioma group from the TCGA and GTEx data sets. **(B, C)** Overall survival analysis **(B)** and disease-free survival analysis **(C)** of the relationship between FCGR2A expression level and survival time from the TCGA database. **(D)** Differences in EHD2 expression between the normal group and the glioma group from the TCGA and GTEX data sets. **(E, F)** Overall survival analysis **(E)** and disease-free survival analysis **(F)** of the relationship between EHD2 expression level and survival time from TCGA database. \*\*\*P<0.001.

Although studies have confirmed that the six selected genes used to construct the signature are related to glioma, they are functionally independent of each other. In particular, EMP3 has been found to upregulate the surface expression of  $\alpha\beta3$  integrin, activate focal adhesion kinase and Src kinase, promote cell migration and invasion, promote tumor growth *in vivo*, and serve as a prognostic evaluation factor for glioma [38, 39]. PLAU can promote cell survival, migration and resistance to targeted cancer therapeutics in cultured glioblastoma cells, and PLAU expression is inversely proportional to patient survival [40]. MVP enhances glioma aggressiveness through the epidermal growth factor receptor (EGFR)/phosphatidylinositol 3-kinase (PI3K) signaling axis [41]. Moreover, compared with normal tissues, RRAS is highly expressed in gliomas. Its overexpression is associated with the early stage of cancer and positively related to the degree of malignancy [42]. The remaining two genes, FCGR2A and EHD2, have not been studied in gliomas. In our research, we found that silencing these genes can inhibit the proliferation, migration and invasion of glioma

cells. Simultaneously, silencing these genes suppresses the expression of mesenchymal marker genes. Overall, the six genes used to construct the risk coefficient model promote the proliferation, migration and invasion of glioma by affecting the EMT process, indicating that they are of particular significance for the prognostic evaluation and treatment of glioma.

In summary, we identified MES-related genes that can be distinguished from the clinical and molecular characteristics of glioma. We believe these 6 MES-related genes are potential prognostic markers or therapeutic targets for glioma patients. Furthermore, we developed a six-MES-related gene expression-based risk signature that could better predict OS for glioma. Functional analysis was carried out, and the effects of two of the genes on the proliferation, migration and invasion of glioma were studied. Nonetheless, the exact mechanism of how these MES-related genes impact the prognosis of glioma is still obscure. Therefore, further research to clarify the underlying mechanism of MES-related genes in glioma is urgently needed.

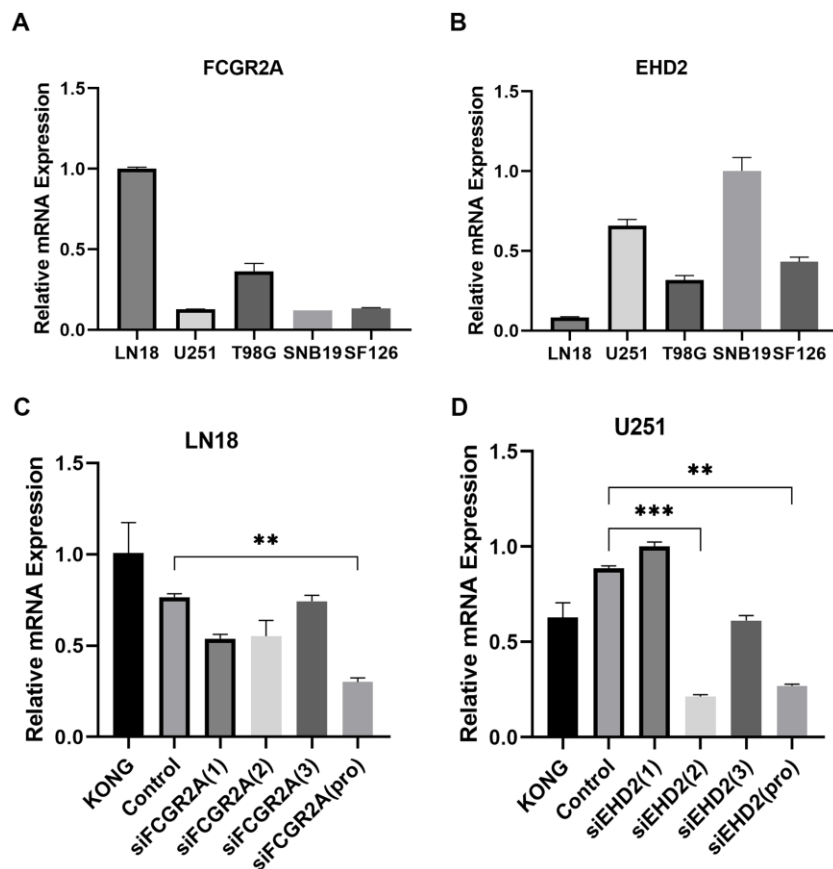


**Figure 7. Selection of cell lines and verification of the silencing effect.** (A) Relative expression of FCGR2A in five cell lines. (B) Relative expression of EHD2 in five cell lines. (C) The LN18 cell line was transfected with three siRNA fragments separately and in combination (pro), and the relative silencing level of FCGR2A. (D) The U251 cell line was transfected with three siRNA fragments separately and in combination (pro), the relative silencing level of EHD2. KONG stands for untreated cell; Control stands for Negative control group. \*\* $P < 0.01$ ; \*\*\* $P < 0.001$ .

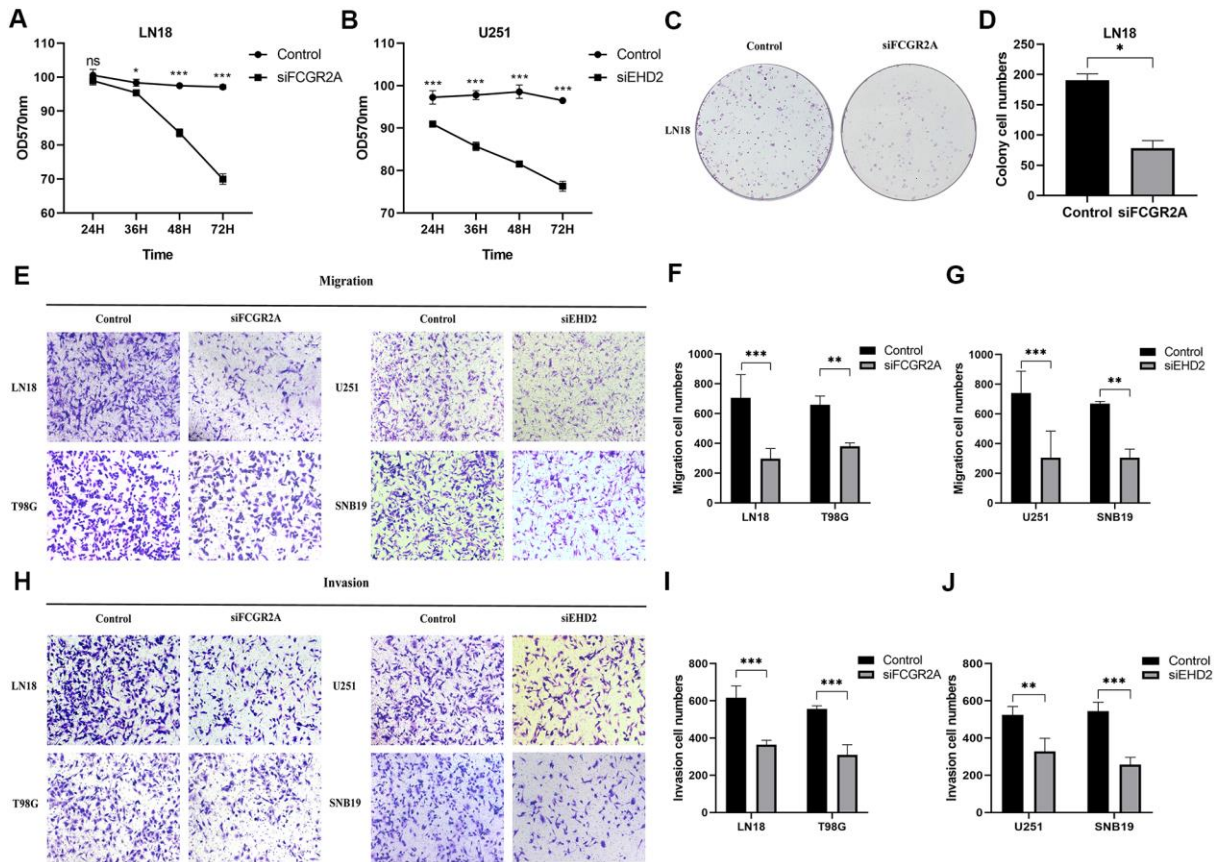


**Figure 8. The effect of glioma cell clone, proliferation, migration and invasion ability after silencing FCGR2A or EHD2.** (A, B) Cell proliferation was measured by the MTT assay for 24 hours up to 72 hours. (C, D) Representative imaging (C) or counting (D) of the colonies formed by LN18 cells after silencing with FCGR2A for 7 days. (E–G) Representative imaging (E) or counting (F, G) of migration assays after silencing FCGR2A and EHD2 in glioma cells. (H–J) Representative imaging (H) or counting (I, J) of invasion assays after silencing FCGR2A and EHD2 in glioma cells. \* $P < 0.05$ ; \*\* $P < 0.01$ ; \*\*\* $P < 0.001$ .

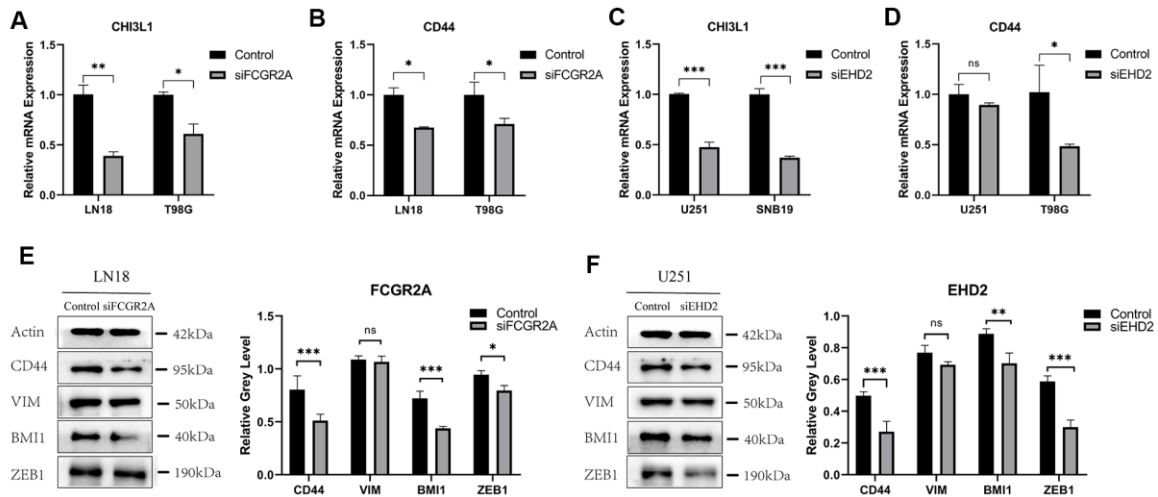


**Figure 9. The relative expression of GBM mesenchymal markers and MES protein markers after FCGR2A or EHD2 silencing.** (A, B) The relative mRNA expression of CHI3L1 and CD44 after silencing FCGR2A. (C, D) The relative mRNA expression of CHI3L1 and CD44 after silencing EHD2. (E) The western blot analysis of CD44, BMI1, VIM and ZEB1 protein markers after silencing FCGR2A. (F) The western blot analysis of CD44, BMI1, VIM and ZEB1 protein markers after silencing EHD2. Ns: no significance; \* $P < 0.05$ ; \*\* $P < 0.01$ ; \*\*\* $P < 0.001$ .



## MATERIALS AND METHODS

### Data sources

Mesenchymal-related gene sets were downloaded from TCGA (<https://xena.ucsc.edu>) and Ivy GAP (<http://glioblastoma.alleninstitute.org>). 1108 normal brain tissue samples were downloaded from GTEx, and patients with glioma were downloaded from the TCGA data portal as a training set, which contained 650 glioma samples after excluding incomplete cases. These data include matched clinical information such as age, gender, survival time and cancer type. To from the testing set, data points with insufficient clinical information were removed from the CGGA (<http://www.cgga.org.cn/index.jsp>) database, and 280 clinical data points in total were obtained. The workflow of this study is shown in Supplementary Figure 1.

### Consensus clustering

We carried out genetic difference analysis with the R programming language (<http://cran.r-project.org>) to obtain the intersecting genes of MES-related genes from the Ivy GAP and TCGA datasets. Twenty-one overlapping MES-related genes were selected, and then differentially expressed genes were identified between normal and glioma samples. Finally, a data set of 15 significant genes was obtained from 21 genes. We used the R package "Consensus Cluster Plus" to perform consensus clustering. The cumulative distribution function (CDF) and consensus matrix were used to evaluate the optimal number of subgroups.

### Bioinformatics analysis

We used univariate and multivariate Cox analyses to screen prognosis-related genes and assess the prediction model of independent prognostic factors. The R programming language was used to perform Lasso regression analysis to obtain the risk score. Through the regression coefficient weighted by the linear combination of genes, the risk score was obtained, and the high-risk group and the low-risk group were obtained based on the median risk score. Kaplan-Meier survival curves were used to analyze the relationship between different groups and survival time. ROC curves were used to judge the sensitivity and specificity of the predictive models to assess prognosis with the R package.

### Functional analysis

The hallmark gene sets, which are part of the MSigDB gene set, were downloaded from the Molecular Signatures Database. Gene set enrichment analysis (GSEA) was used to reveal the signaling pathways most

likely to be affected by the six MES-related genes by using GSEA software (4.0.1) (<http://www.broadinstitute.org/gsea/index.jsp>). Gene Ontology (GO) and Kyoto Encyclopedia of Genes and Genomes (KEGG) analyses used the R programming language to study the cell functions associated with the risk factors composed of six genes in the TCGA database.

### Cell and cell culture

Human glioma cell lines including LN18, U251, T98G, SNB19 and SF126, which were all purchased from the Chinese Academy of Sciences (Shanghai, China). Glioma cells were cultured in Dulbecco's Modified Eagle's medium (DMEM, Hyclone, GE Healthcare Life Sciences) containing 10% fetal bovine serum (FBS, Gibco, Thermo Fisher Scientific, Inc.) in an incubator at 37° C and a carbon dioxide concentration of 5%. After the cells have grown to more than 90%, digest with 0.25% enzyme (C0201; Beyotime, China) to passage cell. Based on this culture state, the medium of the cells was changed every 2 days.

### Cell transfection

FCGR2A and EHD2 siRNAs were designed by RIBOBIO (Guangzhou RiboBio Co.). FCGR2A siRNA included three sequences (siFCGR2A-1 AGGCTGTGC TGAAACTTGA, siFCGR2A-2 GGTCATTGCGACTG CTGTA, and siFCGR2A-3 CTTCAACCATTGAC AGTTT), and the EHD2 siRNA also included three sequences (siEHD2-1 AGACCAGCTTCATCCAGTA, siEHD2-2 GCACGACTTCACCAAGTTT, and siEHD2-3 TGCGAAGATTCAGCTGGAA). Then, we used the siRNAs to silence FCGR2A in LN18 and T98G cell lines and to silence EHD2 in U251 and SNB19 cell lines with the transfection reagent jetPRIME (Poly plus-transfection®). Continue to cultivate for 24 h, then change the medium.

### Total RNA isolation and quantitative real-time polymerase chain reaction (qRT-PCR)

Total RNA was extracted by TRIzol reagent (Invitrogen, Thermo Fisher Scientific) according to the manufacturer's instructions. PrimeScript RT Master Mix (Perfect Real Time) (RR036A; Takara) was used for RNA reverse transcription, and quantitative real-time PCR (qRT-PCR) was performed with TB Green™ Premix Ex Taq™ II (Tli RNaseH Plus) (RR820A; Takara). The total volume of each PCR reaction mixture is 10ul, 45 cycles are performed, denaturation at 95° C for 15 seconds, annealing at 60° C for 30 seconds, and extension at 72° C for 30 seconds. The relative mRNA expression of each gene was calculated using the 2<sup>-ΔΔCt</sup> method. The following PCR primers were used:



FCGR2A forward: 5'-ACTATGGAGACCCAAATGTC TCAG-3'; reverse:5'-GCAAACTGTCAATGGTTGA AGC-3'.

EHD2 forward: 5'-AACCCCTTTCGGAAACACCTT-3'; reverse: 5'-TCGATGATGCTGATGCTCTC-3'.

CHI3L1 forward: 5'-CCCTGGACGGAGAGACAAAC-3'; reverse:5'-GCCTCAACATGTACCCCAACA -3'.

CD44 forward: 5'-CGCCAAACACCCAAAGAAGA-3'; reverse: 5'-TTCCTGCTTGATGACCTCGT -3'.

GAPDH forward: 5'-AGCAAGAGCACAAGAGGAA G-3'; reverse:5'-GGTTGAGCACAGGGTACTTT -3'.

### **Methyl thiazolyl tetrazolium (MTT) assay**

By comparison, 2000 and 4000 cells were plated onto 96-well plates in triplicate for the MTT (3-(4,5-dimethylthiazol-2-yl)-2,5-diphenyltetrazolium bromide) assay. After incubation for 24 h, 36 h, 48 h and 72 h, the medium was replaced, and 10% of the medium volume of MTT dye (ST316; Beyotime, China) was added. Then, the cells were incubated for 4 h. After that, the medium was thoroughly removed, 150  $\mu$ l of dimethyl sulfoxide (DMSO; D8370; Solarbio, China) was added, and the cells were shaken for 10 minutes. After it was fully dissolved, the absorbance at 570nm was measured with Varioskan LUX Multifunctional Microplate Reader (Thermo Scientific, MA, USA).

### **Colony formation assay**

The cells were seeded at a density of 200, 400, and 600 cells per well, repeated at least 3 times in a 6-well plate, and incubated at 37° C for seven days. After that, the cells were fixed with 4% paraformaldehyde (P0099; Beyotime, China) for 25 minutes. Next, the cells were stained with 0.5% crystal violet (C8470; Solarbio) for 15 minutes. Then, the crystal violet was absorbed as much as possible, and the excess crystal violet was gently washed off with PBS. Finally, we observed and took photos on the light microscope at  $\times$ 100 magnification (Olympus IX71, Japan).

### **Transwell migration assay and Matrigel invasion assay**

Twenty-four-well Transwell chambers (29017037; Corning) were used for the Transwell migration assay and invasion assay. Briefly, the upper chamber contained 200  $\mu$ l of serum-free DMEM, and  $2 \times 10^4$  transfected cells were added. Meanwhile, 600  $\mu$ l of DMEM with 30% FBS was placed in the lower well and cultured at 37° C for 24 h, but SNB19 needs to be cultured for 36 h.

Furthermore, an invasion assay was performed by using Matrigel (356234; BD Biosciences) inserts precoated for Matrigel, and  $1 \times 10^5$  cells were plated in each chamber and cultivated at 37° C for 48 h. After incubation, the chambers were fixed with 4% paraformaldehyde for 25 minutes and then stained with 0.5% crystal violet for 15 minutes. Cells remaining on the upper surface of the chamber were gently removed with a cotton swab. The remaining cells were counted under a light microscope at 100X magnification (Olympus IX71, Japan) in four random fields.

### **Western blot analysis**

The protein of glioma cells LN18 and U251 were isolated by RIPA buffer (P0013B; Beyotime) with protease inhibitors cocktail (C00001; TargetMol). Get an equal amount of protein sample from RIPA lysate for Western blot analysis. The protein was separated by SDS-PAGE, and then electro-transfer onto poly-vinylidene difluoride membranes (IPVH00010; Millipore). Then 5% skim milk was blocked for 1.5 hours, and then the primary antibodies were incubated overnight with anti- $\beta$ -actin(1:10,000; #66009-1-Ig; Proteintech Group), anti-BMI1(1:2,000; #66161-1-Ig; Proteintech Group), anti-CD44(1:5,000; #60224-1-Ig; Proteintech Group), anti-Vimentin(1:5,000; #10366-1-AP; Proteintech Group), anti-ZEB1(1:1,000; 21544-1-AP; Proteintech Group), anti-bodies, respectively, at 4° C. Then incubate with the secondary antibody for 1 hour. Protein observation was done using ECL-Chemiluminescence kit (ECL-plus, Thermo Fisher Scientific, Inc.), and then detect the luminescence with a Protein Imager (Find-Do $\times$ 6; Tanon). The relative gray level of western blot was measured by the ImageJ software for Microsoft Windows (National Institute of Health, Bethesda, MD, USA).

### **Statistical analysis**

GraphPad Prism 8 was used for graphing and statistical analysis. ImageJ software for Microsoft Windows was used for the cell number and clone formation counts. R programming language was used to perform the univariate and multivariate Cox regression analyses. Kaplan-Meier curves were used to statistically analyze the difference in survival between the two groups. Student's t-test and the chi-square test were used to assess differences in clinical characteristics between samples grouped by the risk score, and Pearson correlation was used to calculate correlations. Statistical significance was defined as a 2-tailed p value  $< 0.05$ .

### **Data availability statement**

All data included in this study are available upon request by contact with the corresponding author.

## Editorial note

&This corresponding author has a verified history of publications using a personal email address for correspondence.

## Abbreviations

TCGA: The Cancer Genome Atlas; GTEx: Genotype-Tissue Expression; CGGA: Chinese Glioma Genome Atlas; Ivy GAP: Ivy Glioblastoma Atlas Project; GBM: glioblastoma multiforme; EMT: Epithelial-Mesenchymal Transition; MES: mesenchymal subtype; PN: proneural subtype; Prolif: proliferative subtype; GSEA: Gene set enrichment analysis; GO: Gene Ontology; KEGG: Kyoto Encyclopedia of Genes and Genomes; FCGR2A: Fc fragment of IgG receptor IIa; EHD2: EH Domain Containing 2; CHI3L1: Chitinase 3 Like 1; GAPDH: glyceraldehyde-3-phosphate dehydrogenase; CD44: CD44 Molecule; SERPINE1: Serpin Family E Member 1; PDPN: Podoplanin; STAT3: signal transducer and activator of transcription 3; C/EBP $\beta$ : CCAAT Enhancer Binding Protein Beta; TAZ: Tafazzin; EMP3: Epithelial Membrane Protein 3; PLAUR: Plasminogen Activator: Urokinase Receptor; MVP: Major Vault Protein; RRAS: RAS Related; VIM: Vimentin; BMI1: BMI1 Proto-Oncogene; Polycomb Ring Finger; ZEB1: Zinc Finger E-Box Binding Homeobox 1.

## AUTHOR CONTRIBUTIONS

Bing Zhao, Erbao Bian and Zhengwei Zhang conceived and designed the experiments. Zhengwei Zhang, Jie Chen and Xiuhao Huo performed the experiments. Gang Zong, Kebin Huang, Meng Cheng and Libo Sun analyzed the data. Zhengwei Zhang, Jie Chen and Xiaoyu Yue drafted the manuscript. Bing Zhao and Erbao Bian revised the manuscript and was responsible for the whole study.

## ACKNOWLEDGMENTS

The author thanks CGGA network and TCGA network for their contributions.

## CONFLICTS OF INTEREST

The authors declare that there is no conflict of interests.

## FUNDING

This research was funded by the National Natural Science Foundation of China (No. 81972348), Key Research and Development Plan Project of Anhui Province (No.1804h08020270), College Excellent Youth Talent Support Program in Anhui Province

(No.gxypZD2019019), Key Projects of Natural Science Research in Anhui Province (KJ2019A0267), Academic Funding Project for Top Talents in Colleges and Universities in Anhui Province (No. gxbjZD10), Nova Pew Plan of the Second Affiliated Hospital of Anhui Medical University (No.2017KA01), Open Projects of Key Laboratory in Medical Physics and Technology of Anhui Province(LHJJ202001).

## REFERENCES

1. Ostrom QT, Bauchet L, Davis FG, Deltour I, Fisher JL, Langer CE, Pekmezci M, Schwartzbaum JA, Turner MC, Walsh KM, Wrensch MR, Barnholtz-Sloan JS. The epidemiology of glioma in adults: a “state of the science” review. *Neuro Oncol.* 2014; 16:896–913. <https://doi.org/10.1093/neuonc/nou087> PMID:[24842956](https://pubmed.ncbi.nlm.nih.gov/24842956/)
2. Ostrom QT, Gittleman H, Farah P, Ondracek A, Chen Y, Wolinsky Y, Stroup NE, Kruchko C, Barnholtz-Sloan JS. CBTRUS statistical report: primary brain and central nervous system tumors diagnosed in the United States in 2006–2010. *Neuro Oncol.* 2013 (Suppl 2); 15:ii1–56. <https://doi.org/10.1093/neuonc/not151> PMID:[24137015](https://pubmed.ncbi.nlm.nih.gov/24137015/)
3. Jiang T, Mao Y, Ma W, Mao Q, You Y, Yang X, Jiang C, Kang C, Li X, Chen L, Qiu X, Wang W, Li W, et al, and Chinese Glioma Cooperative Group (CGCG). CGCG clinical practice guidelines for the management of adult diffuse gliomas. *Cancer Lett.* 2016; 375:263–73. <https://doi.org/10.1016/j.canlet.2016.01.024> PMID:[26966000](https://pubmed.ncbi.nlm.nih.gov/26966000/)
4. Stupp R, Hegi ME, Mason WP, van den Bent MJ, Taphoorn MJ, Janzer RC, Ludwin SK, Allgeier A, Fisher B, Belanger K, Hau P, Brandes AA, Gijtenbeek J, et al, and European Organisation for Research and Treatment of Cancer Brain Tumour and Radiation Oncology Groups, and National Cancer Institute of Canada Clinical Trials Group. Effects of radiotherapy with concomitant and adjuvant temozolomide versus radiotherapy alone on survival in glioblastoma in a randomised phase III study: 5-year analysis of the EORTC-NCIC trial. *Lancet Oncol.* 2009; 10:459–66. [https://doi.org/10.1016/S1470-2045\(09\)70025-7](https://doi.org/10.1016/S1470-2045(09)70025-7) PMID:[19269895](https://pubmed.ncbi.nlm.nih.gov/19269895/)
5. Styli SS. Novel treatment strategies for glioblastoma. *Cancers (Basel).* 2020; 12:2883. <https://doi.org/10.3390/cancers12102883> PMID:[33049911](https://pubmed.ncbi.nlm.nih.gov/33049911/)
6. Louis DN, Perry A, Reifenberger G, von Deimling A, Figarella-Branger D, Cavenee WK, Ohgaki H, Wiestler OD, Kleihues P, Ellison DW. The 2016 World Health Organization classification of tumors of the central nervous system: a summary. *Acta Neuropathol.* 2016;

- 131:803–20.  
<https://doi.org/10.1007/s00401-016-1545-1>  
PMID:[27157931](https://pubmed.ncbi.nlm.nih.gov/27157931/)
7. Silantyev AS, Falzone L, Libra M, Gurina OI, Kardashova KS, Nikolouzakis TK, Nosyrev AE, Sutton CW, Mitsias PD, Tsatsakis A. Current and future trends on diagnosis and prognosis of glioblastoma: from molecular biology to proteomics. *Cells*. 2019; 8:863.  
<https://doi.org/10.3390/cells8080863> PMID:[31405017](https://pubmed.ncbi.nlm.nih.gov/31405017/)
  8. Verhaak RG, Hoadley KA, Purdom E, Wang V, Qi Y, Wilkerson MD, Miller CR, Ding L, Golub T, Mesirov JP, Alexe G, Lawrence M, O’Kelly M, et al, and Cancer Genome Atlas Research Network. Integrated genomic analysis identifies clinically relevant subtypes of glioblastoma characterized by abnormalities in PDGFRA, IDH1, EGFR, and NF1. *Cancer Cell*. 2010; 17:98–110.  
<https://doi.org/10.1016/j.ccr.2009.12.020>  
PMID:[20129251](https://pubmed.ncbi.nlm.nih.gov/20129251/)
  9. Cancer Genome Atlas Research Network. Comprehensive genomic characterization defines human glioblastoma genes and core pathways. *Nature*. 2008; 455:1061–68.  
<https://doi.org/10.1038/nature07385>  
PMID:[18772890](https://pubmed.ncbi.nlm.nih.gov/18772890/)
  10. Jeanmougin M, Håvik AB, Cekaite L, Brandal P, Sveen A, Meling TR, Ågesen TH, Scheie D, Heim S, Lothe RA, Lind GE. Improved prognostication of glioblastoma beyond molecular subtyping by transcriptional profiling of the tumor microenvironment. *Mol Oncol*. 2020; 14:1016–27.  
<https://doi.org/10.1002/1878-0261.12668>  
PMID:[32171051](https://pubmed.ncbi.nlm.nih.gov/32171051/)
  11. Yoon SJ, Shim JK, Chang JH, Moon JH, Roh TH, Sung KS, Lee JH, Kim EH, Kim SH, Hong YK, Lee SJ, Huh YM, Kang SG. Tumor mesenchymal stem-like cell as a prognostic marker in primary glioblastoma. *Stem Cells Int*. 2016; 2016:6756983.  
<https://doi.org/10.1155/2016/6756983>  
PMID:[26981133](https://pubmed.ncbi.nlm.nih.gov/26981133/)
  12. Carro MS, Lim WK, Alvarez MJ, Bollo RJ, Zhao X, Snyder EY, Sulman EP, Anne SL, Doetsch F, Colman H, Lasorella A, Aldape K, Califano A, Iavarone A. The transcriptional network for mesenchymal transformation of brain tumours. *Nature*. 2010; 463:318–25.  
<https://doi.org/10.1038/nature08712> PMID:[20032975](https://pubmed.ncbi.nlm.nih.gov/20032975/)
  13. Chen J, Li Y, Yu TS, McKay RM, Burns DK, Kernie SG, Parada LF. A restricted cell population propagates glioblastoma growth after chemotherapy. *Nature*. 2012; 488:522–26.  
<https://doi.org/10.1038/nature11287> PMID:[22854781](https://pubmed.ncbi.nlm.nih.gov/22854781/)
  14. Guerra-Rebollo M, Garrido C, Sánchez-Cid L, Soler-Botija C, Meca-Cortés O, Rubio N, Blanco J. Targeting of replicating CD133 and OCT4/SOX2 expressing glioma stem cells selects a cell population that reinitiates tumors upon release of therapeutic pressure. *Sci Rep*. 2019; 9:9549.  
<https://doi.org/10.1038/s41598-019-46014-0>  
PMID:[31267022](https://pubmed.ncbi.nlm.nih.gov/31267022/)
  15. Martinez-Lage M, Lynch TM, Bi Y, Cocito C, Way GP, Pal S, Haller J, Yan RE, Ziober A, Nguyen A, Kandpal M, O’Rourke DM, Greenfield JP, et al. Immune landscapes associated with different glioblastoma molecular subtypes. *Acta Neuropathol Commun*. 2019; 7:203.  
<https://doi.org/10.1186/s40478-019-0803-6>  
PMID:[31815646](https://pubmed.ncbi.nlm.nih.gov/31815646/)
  16. Xia P, Li Q, Wu G, Huang Y. An immune-related lncRNA signature to predict survival in glioma patients. *Cell Mol Neurobiol*. 2021; 41:365–75.  
<https://doi.org/10.1007/s10571-020-00857-8>  
PMID:[32410107](https://pubmed.ncbi.nlm.nih.gov/32410107/)
  17. Tu Z, Wu L, Wang P, Hu Q, Tao C, Li K, Huang K, Zhu X. N6-methyladenosine-related lncRNAs are potential biomarkers for predicting the overall survival of lower-grade glioma patients. *Front Cell Dev Biol*. 2020; 8:642.  
<https://doi.org/10.3389/fcell.2020.00642>  
PMID:[32793593](https://pubmed.ncbi.nlm.nih.gov/32793593/)
  18. Zhou Z, Huang R, Chai R, Zhou X, Hu Z, Wang W, Chen B, Deng L, Liu Y, Wu F. Identification of an energy metabolism-related signature associated with clinical prognosis in diffuse glioma. *Aging (Albany NY)*. 2018; 10:3185–209.  
<https://doi.org/10.18632/aging.101625>  
PMID:[30407923](https://pubmed.ncbi.nlm.nih.gov/30407923/)
  19. Cheng M, Zhang ZW, Ji XH, Xu Y, Bian E, Zhao B. Super-enhancers: A new frontier for glioma treatment. *Biochim Biophys Acta Rev Cancer*. 2020; 1873:188353.  
<https://doi.org/10.1016/j.bbcan.2020.188353>  
PMID:[32112817](https://pubmed.ncbi.nlm.nih.gov/32112817/)
  20. Chai R, Zhang K, Wang K, Li G, Huang R, Zhao Z, Liu Y, Chen J. A novel gene signature based on five glioblastoma stem-like cell relevant genes predicts the survival of primary glioblastoma. *J Cancer Res Clin Oncol*. 2018; 144:439–47.  
<https://doi.org/10.1007/s00432-017-2572-6>  
PMID:[29299749](https://pubmed.ncbi.nlm.nih.gov/29299749/)
  21. Mao P, Joshi K, Li J, Kim SH, Li P, Santana-Santos L, Luthra S, Chandran UR, Benos PV, Smith L, Wang M, Hu B, Cheng SY, et al. Mesenchymal glioma stem cells are maintained by activated glycolytic metabolism involving aldehyde dehydrogenase 1A3. *Proc Natl Acad Sci USA*. 2013; 110:8644–49.  
<https://doi.org/10.1073/pnas.1221478110>

PMID:[23650391](#)

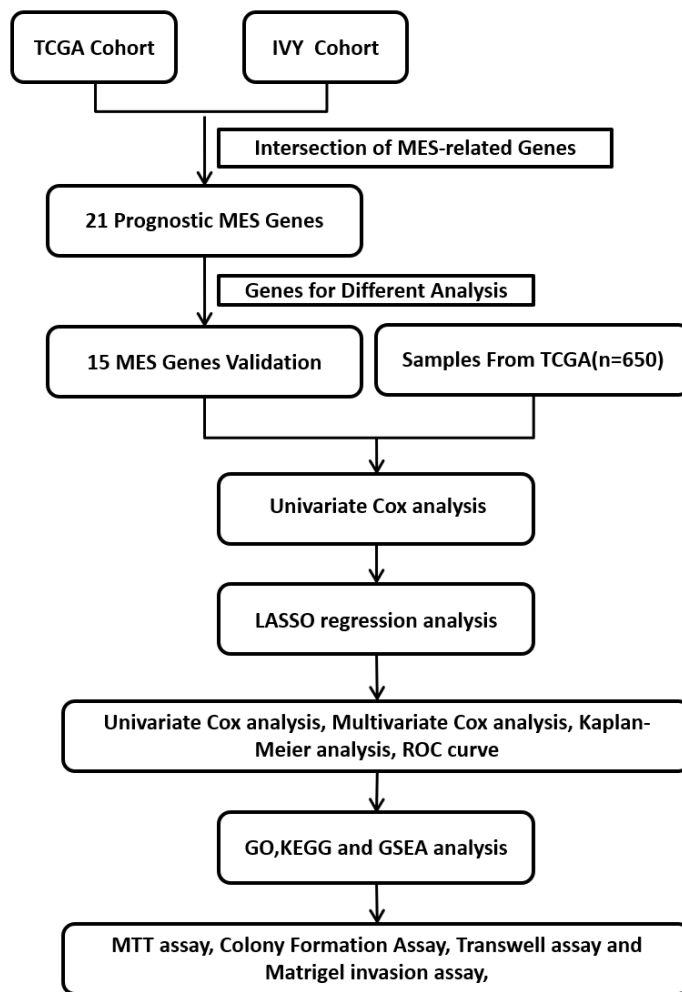
22. Phillips HS, Kharbanda S, Chen R, Forrest WF, Soriano RH, Wu TD, Misra A, Nigro JM, Colman H, Soroceanu L, Williams PM, Modrusan Z, Feuerstein BG, Aldape K. Molecular subclasses of high-grade glioma predict prognosis, delineate a pattern of disease progression, and resemble stages in neurogenesis. *Cancer Cell*. 2006; 9:157–73.  
<https://doi.org/10.1016/j.ccr.2006.02.019>  
PMID:[16530701](#)
23. Bhat KP, Salazar KL, Balasubramanian V, Wani K, Heathcock L, Hollingsworth F, James JD, Gumin J, Diefes KL, Kim SH, Turski A, Azodi Y, Yang Y, et al. The transcriptional coactivator TAZ regulates mesenchymal differentiation in malignant glioma. *Genes Dev*. 2011; 25:2594–609.  
<https://doi.org/10.1101/gad.176800.111>  
PMID:[22190458](#)
24. Yang F, Liu X, Liu Y, Liu Y, Zhang C, Wang Z, Jiang T, Wang Y. miR-181d/MALT1 regulatory axis attenuates mesenchymal phenotype through NF- $\kappa$ B pathways in glioblastoma. *Cancer Lett*. 2017; 396:1–9.  
<https://doi.org/10.1016/j.canlet.2017.03.002>  
PMID:[28286260](#)
25. Niklasson M, Bergström T, Jarvius M, Sundström A, Nyberg F, Haglund C, Larsson R, Westermark B, Segerman B, Segerman A. Mesenchymal transition and increased therapy resistance of glioblastoma cells is related to astrocyte reactivity. *J Pathol*. 2019; 249:295–307.  
<https://doi.org/10.1002/path.5317>  
PMID:[31298733](#)
26. Xia X, Chan KF, Wong GT, Wang P, Liu L, Yeung BP, Ng EK, Lau JY, Chiu PW. Mesenchymal stem cells promote healing of nonsteroidal anti-inflammatory drug-related peptic ulcer through paracrine actions in pigs. *Sci Transl Med*. 2019; 11:eaat7455.  
<https://doi.org/10.1126/scitranslmed.aat7455>  
PMID:[31666403](#)
27. Nduom EK, Wei J, Yaghi NK, Huang N, Kong LY, Gabrusiewicz K, Ling X, Zhou S, Ivan C, Chen JQ, Burks JK, Fuller GN, Calin GA, et al. PD-L1 expression and prognostic impact in glioblastoma. *Neuro Oncol*. 2016; 18:195–205.  
<https://doi.org/10.1093/neuonc/nov172>  
PMID:[26323609](#)
28. Chai RC, Wu F, Wang QX, Zhang S, Zhang KN, Liu YQ, Zhao Z, Jiang T, Wang YZ, Kang CS. m6A RNA methylation regulators contribute to malignant progression and have clinical prognostic impact in gliomas. *Aging (Albany NY)*. 2019; 11:1204–25.  
<https://doi.org/10.18632/aging.101829>  
PMID:[30810537](#)
29. Liu YQ, Chai RC, Wang YZ, Wang Z, Liu X, Wu F, Jiang T. Amino acid metabolism-related gene expression-based risk signature can better predict overall survival for glioma. *Cancer Sci*. 2019; 110:321–33.  
<https://doi.org/10.1111/cas.13878> PMID:[30431206](#)
30. Zhou M, Zhang Z, Zhao H, Bao S, Cheng L, Sun J. An immune-related six-lncRNA signature to improve prognosis prediction of glioblastoma multiforme. *Mol Neurobiol*. 2018; 55:3684–97.  
<https://doi.org/10.1007/s12035-017-0572-9>  
PMID:[28527107](#)
31. Zhang W, Zhang J, Yan W, You G, Bao Z, Li S, Kang C, Jiang C, You Y, Zhang Y, Chen CC, Song SW, Jiang T. Whole-genome microRNA expression profiling identifies a 5-microRNA signature as a prognostic biomarker in Chinese patients with primary glioblastoma multiforme. *Cancer*. 2013; 119:814–24.  
<https://doi.org/10.1002/cncr.27826>  
PMID:[22990979](#)
32. Peng J, Wang X, Ran L, Song J, Luo R, Wang Y. Hypoxia-inducible factor 1 $\alpha$  regulates the transforming growth factor  $\beta$ 1/SMAD family member 3 pathway to promote breast cancer progression. *J Breast Cancer*. 2018; 21:259–66.  
<https://doi.org/10.4048/jbc.2018.21.e42>  
PMID:[30275854](#)
33. Wang Q, Hu B, Hu X, Kim H, Squatrito M, Scarpace L, deCarvalho AC, Lyu S, Li P, Li Y, Barthel F, Cho HJ, Lin YH, et al. Tumor evolution of glioma-intrinsic gene expression subtypes associates with immunological changes in the microenvironment. *Cancer Cell*. 2018; 33:152.  
<https://doi.org/10.1016/j.ccell.2017.12.012>  
PMID:[29316430](#)
34. Zanotto-Filho A, Gonçalves RM, Klafke K, de Souza PO, Dillenburg FC, Carro L, Gelain DP, Moreira JC. Inflammatory landscape of human brain tumors reveals an NF $\kappa$ B dependent cytokine pathway associated with mesenchymal glioblastoma. *Cancer Lett*. 2017; 390:176–87.  
<https://doi.org/10.1016/j.canlet.2016.12.015>  
PMID:[28007636](#)
35. Jhaveri N, Chen TC, Hofman FM. Tumor vasculature and glioma stem cells: contributions to glioma progression. *Cancer Lett*. 2016; 380:545–51.  
<https://doi.org/10.1016/j.canlet.2014.12.028>  
PMID:[25527451](#)
36. Pradella D, Naro C, Sette C, Ghigna C. EMT and stemness: flexible processes tuned by alternative splicing in development and cancer progression. *Mol Cancer*. 2017; 16:8.

- <https://doi.org/10.1186/s12943-016-0579-2>  
PMID:[28137272](https://pubmed.ncbi.nlm.nih.gov/28137272/)
37. Quezada C, Torres Á, Niechi I, Uribe D, Contreras-Duarte S, Toledo F, San Martín R, Gutiérrez J, Sobrevia L. Role of extracellular vesicles in glioma progression. *Mol Aspects Med.* 2018; 60:38–51.  
<https://doi.org/10.1016/j.mam.2017.12.003>  
PMID:[29222067](https://pubmed.ncbi.nlm.nih.gov/29222067/)
38. Gao YF, Zhu T, Mao CX, Liu ZX, Wang ZB, Mao XY, Li L, Yin JY, Zhou HH, Liu ZQ. PPIC, EMP3 and CHI3L1 are novel prognostic markers for high grade glioma. *Int J Mol Sci.* 2016; 17:1808.  
<https://doi.org/10.3390/ijms17111808>  
PMID:[27801851](https://pubmed.ncbi.nlm.nih.gov/27801851/)
39. Ernst A, Hofmann S, Ahmadi R, Becker N, Korshunov A, Engel F, Hartmann C, Felsberg J, Sabel M, Peterziel H, Durchdewald M, Hess J, Barbus S, et al. Genomic and expression profiling of glioblastoma stem cell-like spheroid cultures identifies novel tumor-relevant genes associated with survival. *Clin Cancer Res.* 2009; 15:6541–50.  
<https://doi.org/10.1158/1078-0432.CCR-09-0695>  
PMID:[19861460](https://pubmed.ncbi.nlm.nih.gov/19861460/)
40. Gilder AS, Natali L, Van Dyk DM, Zalfa C, Banki MA, Pizzo DP, Wang H, Klemke RL, Mantuano E, Gonias SL. The urokinase receptor induces a mesenchymal gene expression signature in glioblastoma cells and promotes tumor cell survival in neurospheres. *Sci Rep.* 2018; 8:2982.  
<https://doi.org/10.1038/s41598-018-21358-1>  
PMID:[29445239](https://pubmed.ncbi.nlm.nih.gov/29445239/)
41. Lötsch D, Steiner E, Holzmann K, Spiegl-Kreinecker S, Pirker C, Hlavaty J, Petznek H, Hegedus B, Garay T, Mohr T, Sommergruber W, Grusch M, Berger W. Major vault protein supports glioblastoma survival and migration by upregulating the EGFR/PI3K signalling axis. *Oncotarget.* 2013; 4:1904–18.  
<https://doi.org/10.18632/oncotarget.1264>  
PMID:[24243798](https://pubmed.ncbi.nlm.nih.gov/24243798/)
42. Gutierrez-Erlandsson S, Herrero-Vidal P, Fernandez-Alfara M, Hernandez-Garcia S, Gonzalo-Flores S, Mudarra-Rubio A, Fresno M, Cubelos B. R-RAS2 overexpression in tumors of the human central nervous system. *Mol Cancer.* 2013; 12:127.  
<https://doi.org/10.1186/1476-4598-12-127>  
PMID:[24148564](https://pubmed.ncbi.nlm.nih.gov/24148564/)

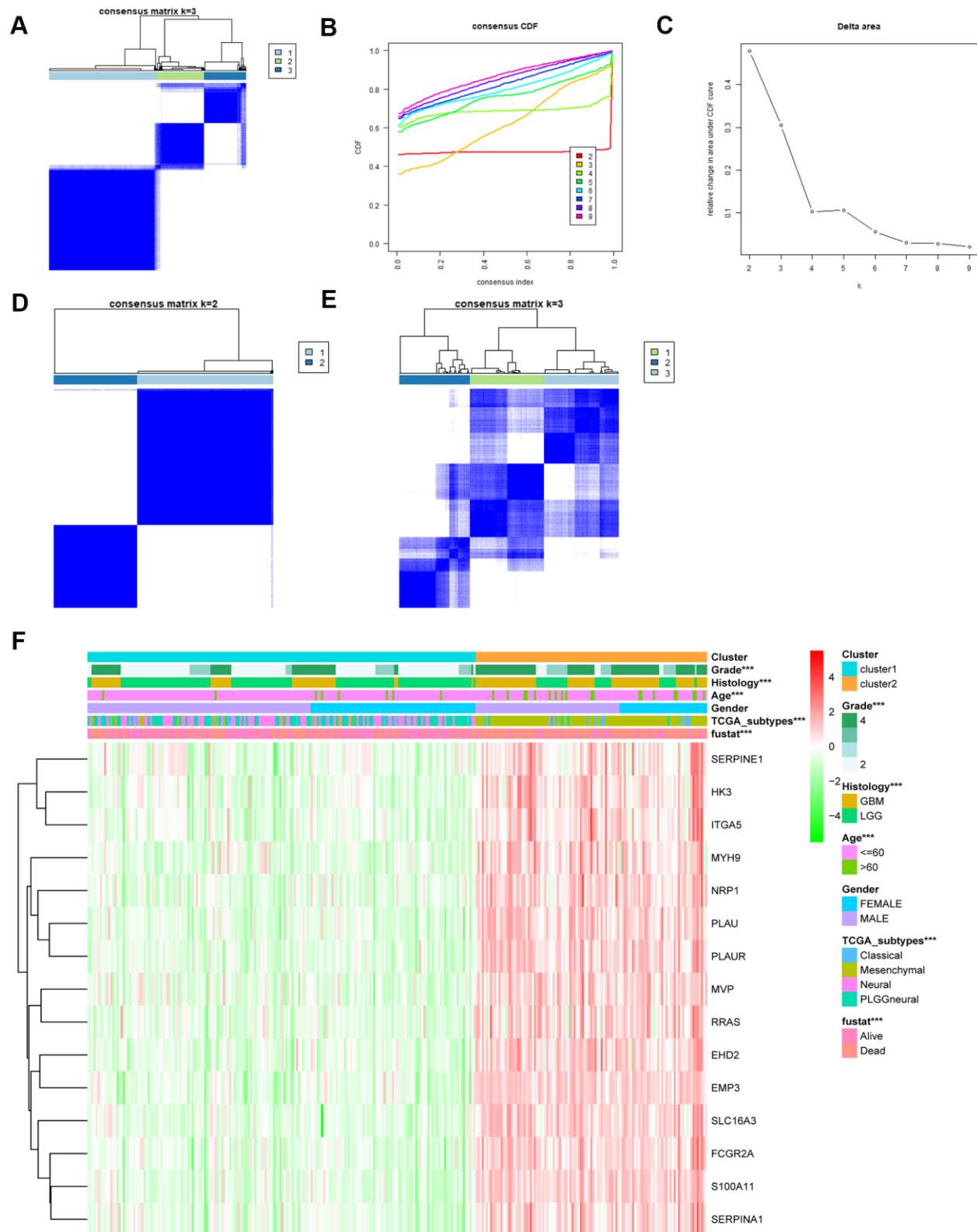


## SUPPLEMENTARY MATERIALS

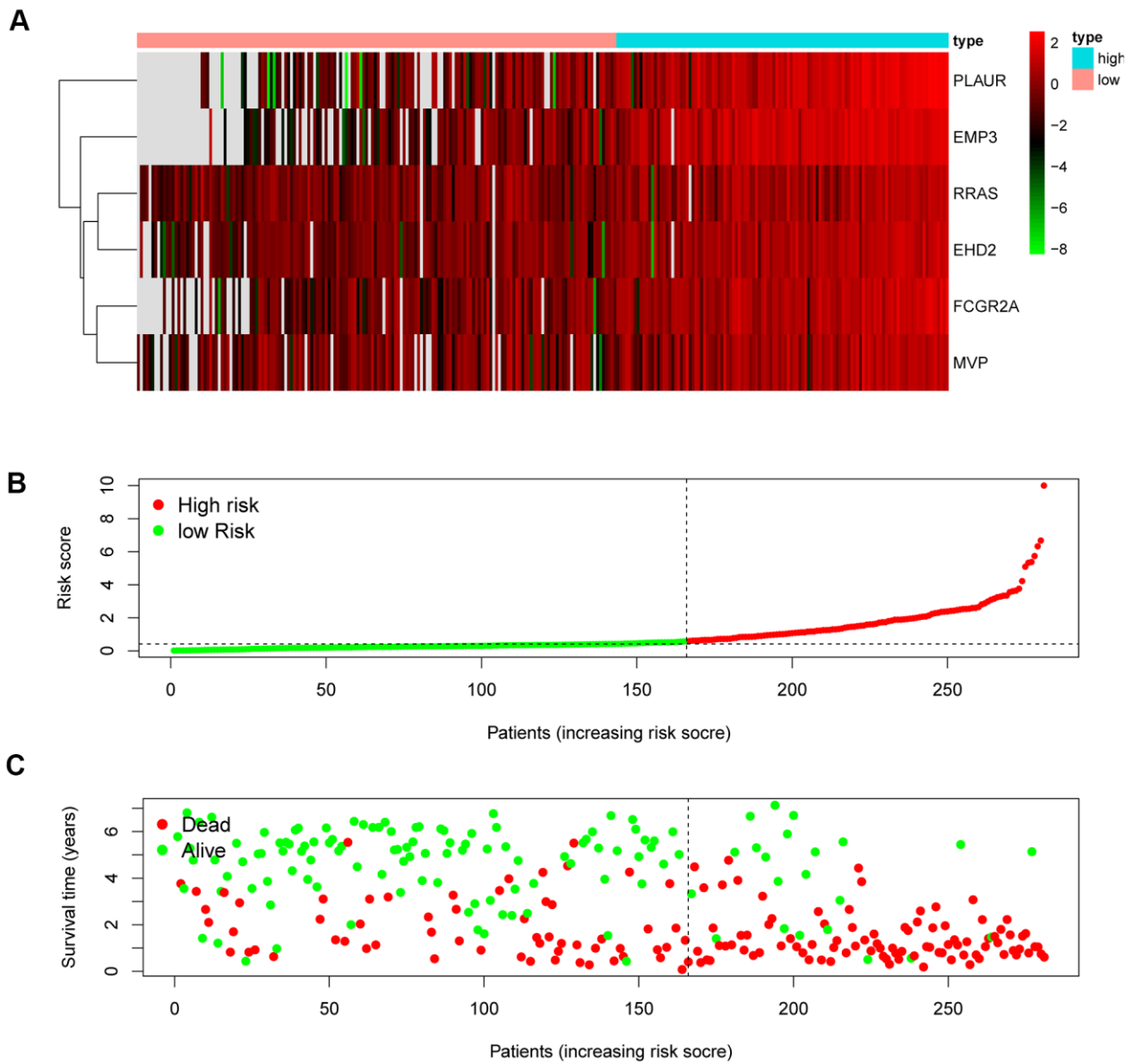
### Supplementary Figures



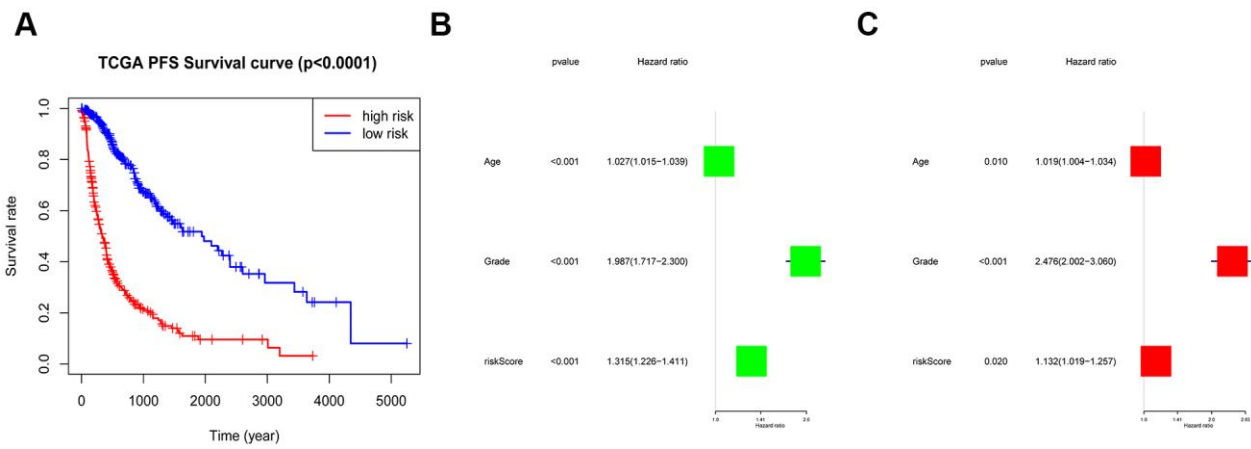
Supplementary Figure 1. The workflow of this study: data collection, analysis, and validation.



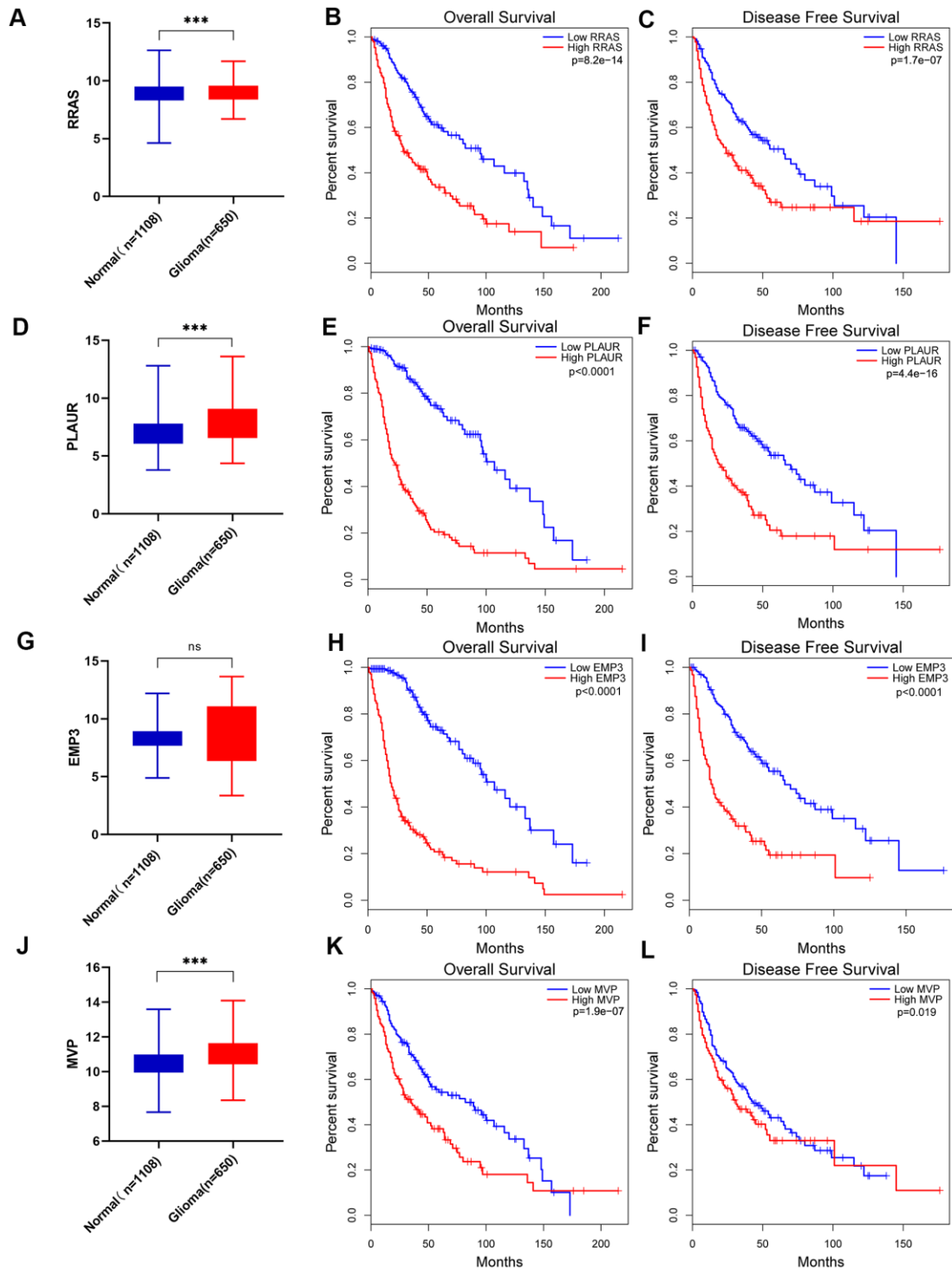
**Supplementary Figure 2. Stratification and verification of glioma based on 15 MES-related genes in the CGGA cohort.** (A) Consensus clustering matrix of 650 TCGA samples for  $k = 3$ . (B) Relative change in the area under the CDF curve for  $k = 2$  to  $k = 9$  in the testing set. (C) Consensus clustering CDF for  $k = 2$  to  $k = 9$  in the testing set. (D, E) Consensus clustering matrix of 280 CGGA samples for  $k = 2$  and  $k = 3$ . (F) Heat map of MES-related genes between CGGA cluster 1 and cluster 2 used to verify consensus clustering based on TCGA. CDF, cumulative distribution function; \*\* $P < 0.01$ ; \*\*\* $P < 0.001$ .



**Supplementary Figure 3. Verification of the 6-gene risk signature in CGGA datasets.** (A) Heat map shows the expression difference of six MES-related genes between the high-risk group and the low-risk group. (B) Risk curve represents the risk score and distribution of 280 cases from the CGGA database. (C) The survival status graph shows the difference in survival time of 280 cases from the CGGA database (each point represents a sample, B, C).

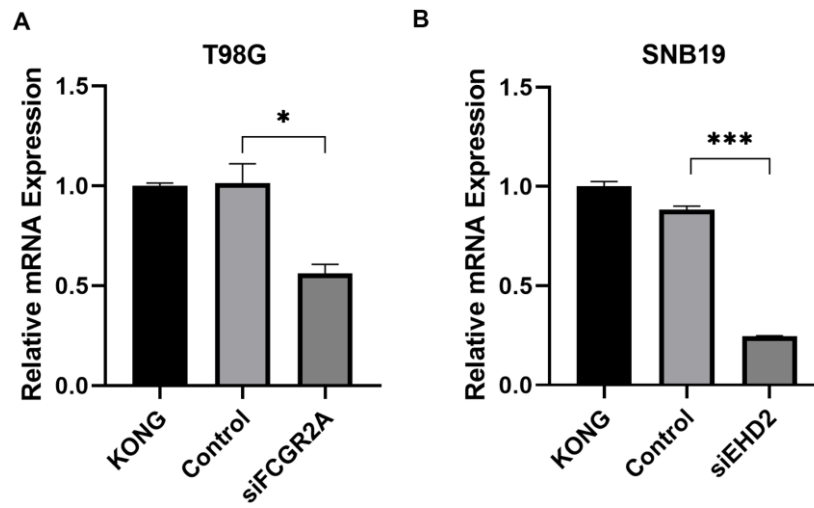


**Supplementary Figure 4. CGGA confirms the independent prognostic value of the risk score.** (A) Progression-free survival analysis between the high- and low-risk groups in the TCGA cohort. (B) Univariate Cox regression analysis of clinical pathologic features for OS in the CGGA cohort. (C) Multivariate Cox regression analysis of clinical pathologic features for OS in the CGGA cohort.

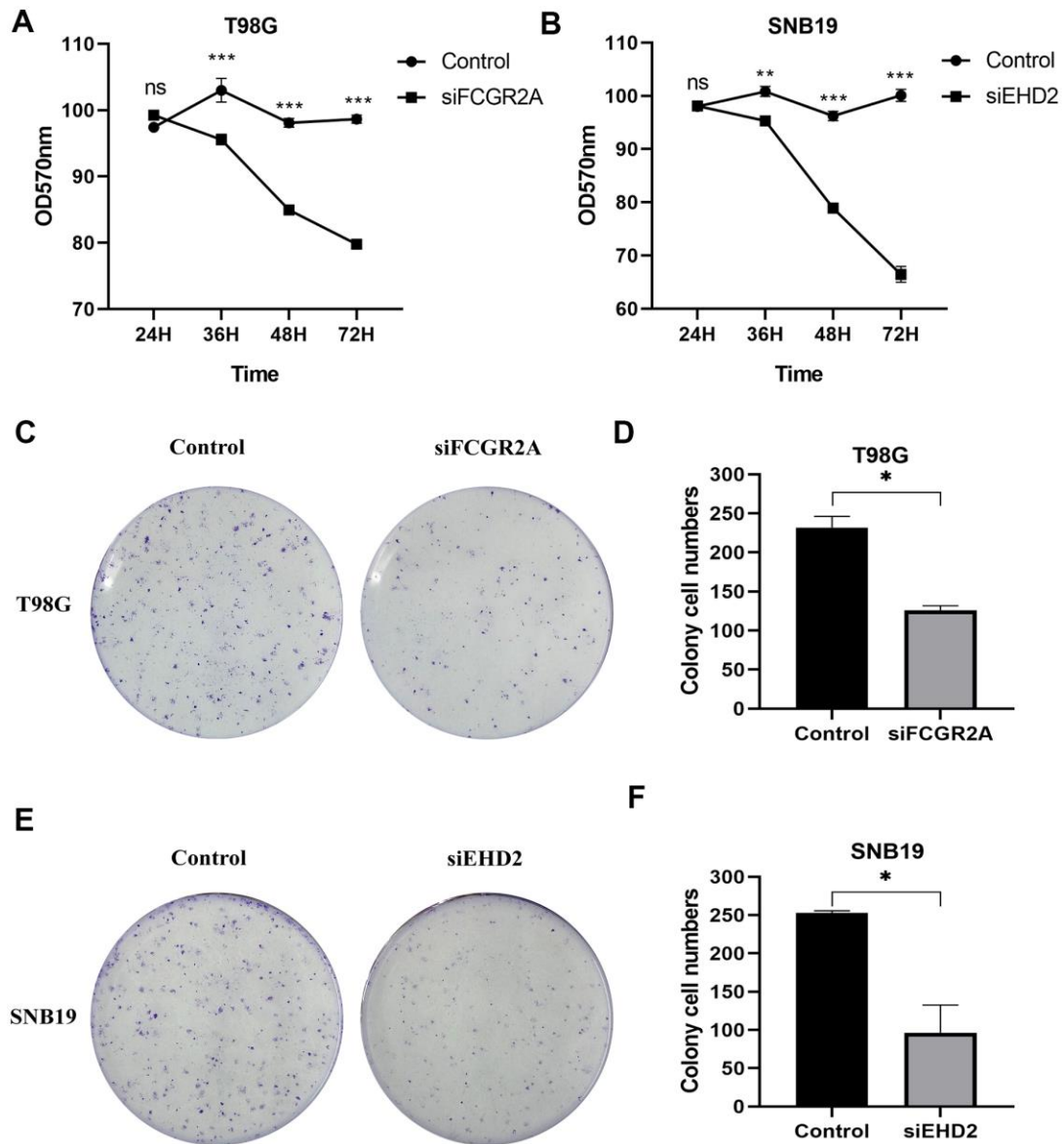


**Supplementary Figure 5. RRAS, PLAUR, EMP3 and MVP gene expression differences and survival rate differences.** (A) Differences in RRAS expression between the normal group and the glioma group from the TCGA and GTEX data. (B, C) Overall survival analysis (B) and disease-free survival analysis (C) of the relationship between RRAS expression level and survival time from the TCGA database. (D) Differences in PLAUR expression between the normal group and the glioma group from the TCGA and GTEX data. (E, F) Overall survival analysis (E) and disease-free survival analysis (F) of the relationship between PLAUR expression level and survival time from the TCGA database. (G) Differences in EMP3 expression between the normal group and the glioma group from the TCGA and GTEX data. (H, I) Overall survival analysis (H) and disease-free survival analysis (I) of the relationship between EMP3 expression level and survival time from the TCGA database. (J) Differences in MVP expression between the normal group and the glioma group from the TCGA and GTEX data. (K, L) Overall survival analysis (K) and disease-free survival analysis (L) of the relationship between MVP expression level and survival time from the TCGA database. Ns: no significance; \*\*\*P<0.001.





**Supplementary Figure 6.** The effect of FCGR2A being silenced by siFCGR2A (pro) in T98G (A) and the effect of EHD2 being silenced by siEHD2 (2) in SNB19 (B). KONG stands for untreated cell; Control stands for Negative control group. \* $P < 0.05$ ; \*\*\* $P < 0.001$ .



**Supplementary Figure 7. The effect of glioma cell clone and proliferation ability after silencing FCGR2A or EHD2.** (A, B) Cell proliferation was measured by MTT assay for 24 hours up to 72 hours. (C, D) Representative imaging (C) or counting (D) of the colonies formed by T98G cells after silencing with FCGR2A for 9 days. (E, F) Representative imaging (E) or counting (F) of the colonies formed by SNB19 cells after silencing with EHD2 for 7 days. Ns: no significance; \*P<0.05; \*\*P<0.01; \*\*\*P<0.001.